The American Journal of Pathology, Vol. 184, No. 4, April 2014

The American Journal of
PATHOLOGY
ajp.amjpathol.org

MUSCULOSKELETAL PATHOLOGY

Altered Macrophage Phenotype Transition Impairs Skeletal Muscle Regeneration

Hanzhou Wang,* David W. Melton,*†‡ Laurel Porter,* Zaheer U. Sarwar,* Linda M. McManus,§‡ and Paula K. Shireman*‡¶

From the Departments of Surgery, Cellular and Structural Biology,† and Pathology,§ and the Sam and Ann Barshop Institute for Longevity and Aging Studies,‡ University of Texas Health Science Center, San Antonio; and The South Texas Veterans Health Care System,¶ San Antonio, Texas*

Accepted for publication December 26, 2013.

Address correspondence to Paula K. Shireman, M.D., Department of Surgery, University of Texas Health Science Center, San Antonio, 7703 Floyd Curl Dr., MC 7741, San Antonio, TX 78229-3900. E-mail: shireman@uthscsa.edu.

Monocyte/macrophage polarization in skeletal muscle regeneration is ill defined. We used CD11b-diphtheria toxin receptor transgenic mice to transiently deplete monocytes/macrophages at multiple stages before and after muscle injury induced by cardiotoxin. Fat accumulation within regenerated muscle was maximal when ablation occurred at the same time as cardiotoxin-induced injury. Early ablation (day 1 after cardiotoxin) resulted in the smallest regenerated myofiber size together with increased residual necrotic myofibers and fat accumulation. However, muscle regeneration after late (day 4) ablation was similar to controls. Levels of inflammatory cells in injured muscle following early ablation and associated with impaired muscle regeneration were determined by flow cytometry. Delayed, but exaggerated, monocyte [$CD11b^+(CD90/B220/CD49b/NK1.1/Ly6G)^-(F4/80/I\text{-}Ab/CD11c)^-Ly6C^{+/-}$] accumulation occurred; interestingly, $Ly6C^+$ and $Ly6C^-$ monocytes were present concurrently in ablated animals and control mice. In addition to monocytes, proinflammatory, $Ly6C^+$ macrophage accumulation following early ablation was delayed compared to controls. In both groups, $CD11b^+F4/80^+$ cells exhibited minimal expression of the M2 markers CD206 and CD301. Nevertheless, early ablation delayed and decreased the transient accumulation of $CD11b^+F4/80^+Ly6C^-CD301^-$ macrophages; in control animals, the later tissue accumulation of these cells appeared to correspond to that of anti-inflammatory macrophages, determined by cytokine production and arginase activity. In summary, impairments in muscle regeneration were associated with exaggerated monocyte recruitment and reduced $Ly6C^-$ macrophages; the switch of macrophage/monocyte subsets is critical to muscle regeneration. *(Am J Pathol 2014, 184: 1167–1184; http://dx.doi.org/10.1016/j.ajpath.2013.12.020)*

Skeletal muscle has a remarkable capacity for regeneration with a complex injury/repair process that includes inflammation, myofiber regeneration, and angiogenesis. The careful orchestration of inflammatory cells and resident muscle stem cells, also known as satellite cells, is vital to skeletal muscle regenerative capacity.[1,2]

Macrophages are unique effector cells in innate immunity that play critical roles in the maintenance of tissue homeostasis. Monocytes/macrophages are major inflammatory cell populations recruited into injured skeletal muscle. Mouse monocytes comprise two phenotypically distinct subsets in blood: $Ly6C^{hi/+}$ cells and $Ly6C^{lo/-}$ cells.[3–5] Although some groups suggest that $Ly6C^{hi/+}$ monocytes are solely recruited into injured tissue and further become $Ly6C^{lo/-}$ monocytes within the tissue,[3,4,6,7] others have suggested that $Ly6C^{lo/-}$ monocytes can also be recruited as a second wave to the injury site after the immediate response by $Ly6C^{hi/+}$ cells.[8,9] Swirski et al[5] further characterized and expanded the definition of $Ly6C^{hi}$ and $Ly6C^{lo}$ monocyte subsets in the blood [specifically, $CD11b^+(F480, I\text{-}Ab, CD11c)^{lo}(CD90, B220, CD49b, NK1.1, Ly6G)^{lo}Ly6C^{hi/lo}$], which were shown to be derived from splenic reserves and recruited to injured myocardium following a myocardial infarction. However, the propensity of $Ly6C^{hi/+}$ and $Ly6C^{lo/-}$ monocytes to differentiate into specific macrophage polarization states (ie, M1 or M2) has not been established. Ramachandran et al[6]

Supported by NIH NHLBI grants R01 HL074236 and F30 HL110743, NIH NCATS grant UL1TR001120, NIH NCI grant P30 CA054174 [to the Core Flow Cytometry Facility (Cancer Therapy & Research Center) of the University of Texas Health Science Center, San Antonio] and Veterans Administration Merit Review grant 1I01BX001186.

Disclosures: None declared.

http://dx.doi.org/10.1016/j.ajpath.2013.12.020

provided evidence that Ly6C^{hi} monocytes were recruited to injured liver and further differentiated into both Ly6C^{hi} and Ly6C^{lo} macrophages. Interestingly, many groups have characterized the Ly6C$^{hi/+}$ monocytes/macrophages as proinflammatory, primarily by their production/expression of proinflammatory cytokines/chemokines such as chemokine ligand-2 [*Ccl2*, also known as monocyte chemoattractant protein-1 (Mcp-1)],[5,6] *Cxcl10* [interferon-γ–induced protein 10 (*Ip-10*)],[6] inducible nitric oxide synthase (iNOS),[10] tumor necrosis factor-α (TNF-α)[7,8,10,11], IL-12,[10] *Cxcl2* [macrophage inflammatory protein-2 (*Mip-2*)],[3] *Il-1β*,[3,7] and vascular endothelial growth factor (VEGF).[5] These groups have also characterized Ly6C$^{lo/-}$ monocytes/macrophages as anti-inflammatory by their production/expression of anti-inflammatory cytokine/chemokines, growth factors, or other markers such as *Ccl22* (*Mdc*),[3] *Ccl17* (*Tarc*),[3] *Il-4*,[5] IL-10,[5,7] transforming growth factor-β (*Tgf-β*),[7] arginase-1 (*Arg1*),[6,12] resistin-like alpha [*Retnla*, also known as found in inflammatory zone-1 (*Fizz-1*)],[6] insulin-like growth factor-1 (*Igf-1*),[3,6] and platelet-derived growth factor-β (*Pdgf-β*).[3] Whereas Ly6C^{+} cells have a short half-life during tissue damage,[4] Ly6C^{-} cells remain in the circulation for longer periods and traffic into peripheral tissues under noninflammatory conditions.[4,13] The dynamics of Ly6C$^{hi/+}$ and Ly6C$^{lo/-}$ monocyte infiltration into injured skeletal muscle and their propensity to contribute to proinflammatory and anti-inflammatory macrophages in this tissue remain to be fully explored.

Although monocytes are recruited to injured tissues, resident macrophages also exist in tissue and play a role in inflammation. Brigitte et al[14] found that resident macrophages form a centripetal migration pathway for recruited leukocytes by producing two chemokines, KC and MCP-1. Two studies selectively ablated resident macrophages using the human diphtheria toxin receptor (DTR) present on CD11b-expressing cells (ie, monocytes/macrophages/neutrophils). One study showed that the intraperitoneal injection of diphtheria toxin (DT) in a CD11b-DTR mouse could ablate resident macrophages in the kidney and ovary, but not the hepatic sinusoidal nor alveolar macrophages.[15] By using a chimeric mouse, CD11b-DTR host with green fluorescent protein (GFP) donor bone marrow (BM), another group[14] demonstrated a reduction in the resident macrophage population in skeletal muscle with intravenous DT treatment. Consequently, a reduction in the recruited GFP^{+} population 1 day after muscle injury compared to control was observed.[14] However, as the transplanted BM was GFP^{+}, it is unclear whether this recruitment deficit was present in the neutrophil population (the primary myeloid cell recruited at day 1), whether this affected macrophage recruitment at any time points along muscle regeneration, or whether this had any effect on the regeneration of the muscle. Regardless, the essential role of ablation of resident macrophages in skeletal muscle regeneration remains elusive.

The concept that macrophages are crucial in muscle regeneration is supported by growing experimental evidence. Firstly, several different methods have been used to deplete monocytes/macrophages to investigate their role in skeletal muscle regeneration. This includes injecting antibodies against F4/80,[16] CD11b,[17,18] macrophage colony-stimulating factor (M-CSF) receptor,[19] or clodronate-containing liposomes[1]; all of these experiments demonstrated that monocyte/macrophage depletion impaired skeletal muscle regeneration. Secondly, mice deficient in *Mcp-1* (also known as *Ccl2*) or the MCP-1 receptor, CC chemokine receptor 2 (*Ccr2*), demonstrated a remarkable decrease in monocyte/macrophage infiltration in association with impaired skeletal muscle regeneration.[20–24] Most importantly, the poor capacity of skeletal muscle regeneration in *Ccr2*$^{-/-}$ mice was restored by transplantation with BM-derived cells from wild-type mice.[25] Thus, *Ccr2* expression by BM-derived cells is critical in skeletal muscle regeneration, an observation that strongly supports the essential role for monocytes/macrophages in this dynamic process.

Macrophages exhibit remarkable plasticity and are physiologically diverse in response to environmental cues. Extensive *in vitro* studies defined two phenotypically different macrophage subsets by activation state.[26–29] Classically activated, or M1 macrophages, obtained by lipopolysaccharide treatment alone or in combination with IFN-γ, secrete proinflammatory cytokines, such as TNF-α, and increased iNOS activity, resulting in the production of reactive oxygen species. Alternatively activated, or M2 macrophages, are activated by IL-4 treatment. M2 macrophages express high *Arg1*, *Ym1*, *Fizz1*,[12] the mannose receptor (CD206), and CD301.[2,30,31] Multiple variants based on different stimuli have been described and designated as M2a, M2b, and M2c,[26,27] or as wound healing and regulatory macrophages.[28]

Monocyte and macrophage subsets also exist in injured skeletal muscle. Following injury, proinflammatory and anti-inflammatory monocytes/macrophages sequentially accumulated in muscle. Initial monocyte/macrophage populations were associated with the production of proinflammatory cytokines and removal of necrotic tissue. These initial populations were replaced by monocytes/macrophages that were associated with the production of anti-inflammatory cytokines and tissue repair.[7,32] In rats, M1 and M2 subsets were defined as ED1^{+} and ED2^{+} macrophages, respectively.[33,34] Although these studies suggest that different monocyte/macrophage subsets are associated with different stages of skeletal muscle regeneration, the kinetics and influence of different monocyte/macrophage subsets in skeletal muscle regeneration remain to be determined.

DTR transgenic mice have been used to study the effects of monocyte/macrophage ablation on tissue injury and repair.[7,15,35,36] DT binds to the heparin-binding epidermal growth factor–like growth factor (hbEGF) receptor (also known as DTR) followed by internalization, rapidly inducing apoptosis in both dividing and terminally differentiated cells.[37] DT exhibits 1×10^4 less affinity in normal mouse cells compared to human cells.[38] Thus, tissue-specific transgenic expression of human hbEGF (DTR)

confers DT sensitivity to murine cells, such as dendritic cells, vascular smooth muscle cells, or monocytes/macrophages.[15,39,40] CD11b-DTR mice express a transgene containing a human DTR under the control of the CD11b promoter that is constitutively expressed in monocytes and macrophages. Ablation studies in peritoneal populations revealed specific ablation of F4/80$^+$ populations in CD11b-DTR mice that were not affected when DT was injected into wild-type mice. Additionally, other population cell numbers such as of T cells, B cells, and granulocytes in the spleen and peritoneal cavity were not affected by DT administration in CD11b-DTR mice.[41] Therefore, monocytes/macrophages can be transiently and specifically ablated by treatment with a single dose of DT.

In this study, we used DTR transgenic mice on a FVB background (CD11b-DTR) to transiently ablate monocytes/macrophages at different time points following injury to investigate the effect of monocyte and macrophage subsets on skeletal muscle regeneration. Ablating early infiltrating monocytes/macrophages impaired skeletal muscle regeneration, whereas later ablation had a minimal effect on this tissue response to injury.

Materials and Methods

Experimental Animals

Founder CD11b-DTR breeding mice were purchased from Jackson Laboratory (Jackson Laboratory stock #05515; Bar Harbor, ME) and were bred at the Audie Murphy Veterans Hospital. Four- to 6-month-old male mice were used in this study. All procedures complied with the National Institutes of Health regulations and were regularly reviewed by the institutional animal care and use committees of the University of Texas Health Science Center at San Antonio and the South Texas Veterans Health Care System, San Antonio, TX.

Mouse Cardiotoxin Model

Myonecrosis was induced by the intramuscular injection of cardiotoxin (CTX) (Calbiochem, San Diego, CA) as previously described.[22] CTX destroys muscle fibers but preserves the muscle fiber basal lamina, nerves, blood vessels, and satellite cells.[42] In brief, two 50-μL injections of CTX (2.5 μmol/L in normal saline) were delivered uniformly into the muscles of the right hindlimb anterior compartment; the right hindlimb posterior compartment received four 50-μL CTX injections. The left hindlimb was injected in a similar manner with identical volumes of normal saline. Baseline mice did not receive any injection and were used as controls. For flow cytometry experiments, mice were administered CTX injections into both hindlimbs.

DT/Diphtheria Toxin Mutant Administration

CD11b-DTR mice were treated with DT, 15 ng/g body weight (List Biological Laboratories, Campbell CA), by intraperitoneal injection. Control CD11b-DTR mice received the same amount of mutated DT (DTm) (List Biological Laboratories), which does not bind to the DTR. For the current study, we determined the optimal dose schedule of DT administration that could be safely used to evaluate skeletal muscle regeneration allowing long-term survival of the mice. Mice were divided into groups and received one dose of DT from 15 to 35 ng/g body weight in 5 ng/g steps in dosages between groups. The higher DT dose group (range, 20 to 35 ng/g body weight) resulted in 75% mortality at days 7 to 12 after DT injection. By contrast, mice in the low-dose DT group (15 ng/g body weight) had a mortality rate of 17% and could therefore be used in experiments requiring a 21-day time point. To determine whether multiple doses could be used, a cohort of mice was given two to three doses of DT (10 to 15 ng/g body weight) at least 1 week apart. Most of these mice died at days 7 to 12. Therefore, we chose a single dose of 15 ng/g body weight DT to ablate CD11b$^+$ cells. These conditions allowed for the survival of the animals through the course of the experiment (21 days) while temporarily ablating the monocyte/macrophage population within a specific time frame. Previous work and our results in the kinetics of DT ablation of monocyte/macrophage populations in multiple tissues including regenerating skeletal muscle and blood indicate that ablation occurs within 12 hours, lasts 24 hours, with recovery generally occurring 48 hours after DT administration.[7,15] Single injections of DT were administered at various times (−0.5, 0, 1, 2, and 4 days) relative to the injection of CTX to transiently ablate monocyte/macrophages at different time points during skeletal muscle regeneration.

Histology and Histomorphometry

Mice were sacrificed and the tibialis anterior (TA) muscles were collected and placed in 10% neutral-buffered formalin before routine paraffin embedding. For morphometric analysis, 2- to 3-μm cross sections of the mid-portion of the anterior compartment specimen were deparaffinized and stained with H&E. For injury and residual necrosis assessment, slides were scanned using a model ScanScope CS system (Aperio Technologies, Vista, CA) to create a digital image of the entire anterior compartment for further analysis by NIS Elements software version 3.0 (Nikon Instruments, Melville, NY).

Myofiber cross-sectional area, fat area (%), and capillary density in TA muscle were determined as previously described.[20] In brief, the cross-sectional area (μm^2) of myofibers was determined by measurement of individual myofibers in digitized images of a given TA muscle. Only regenerated fibers were measured in the post-CTX specimen, whereas mature myofibers with peripherally located nuclei were measured in the baseline specimen. For morphometric analyses, within each section, four nonoverlapping areas of the TA muscle were digitally captured (×20 magnification) using phase contrast microscopy; areas containing large

blood vessels or fibrous tissue bands between muscle bundles were excluded, and care was taken to avoid TA specimens with tangential or longitudinal presentation of myofibers. For each histomorphometric parameter, results from all images derived from a given section were averaged to obtain a single value for each animal. Fat area (%) was calculated after manual outline of the intermuscular fat area and division by the total area of the TA image. Using digitally captured images of the entire TA in cross section, the total area of injury for a given TA muscle was defined as the area of regenerated myofibers with centrally located nuclei combined with the area of residual necrotic myofibers. Percent muscle injury was calculated as the entire area of injury relative to the entire cross-sectional area of TA. Percent residual necrosis was calculated as the area of necrotic myofibers relative to the entire area of injury.

Capillary counts were evaluated after treatment of deparaffinized cross sections of TA muscle with a biotinylated lectin, *Griffonia (Banderaea) simplicifolia* lectin I (Vector Laboratories, Burlingame, CA), at dilution 1:50 followed by streptavidin-horseradish peroxidase and incubation in diaminobenzidine/hydrogen peroxide to identify endothelial cells as previously described.[20] Only capillaries associated with myofibers were included and were expressed as capillaries per fiber. In addition, after subtracting the areas of fat, fibrosis, and residual necrosis from the total area, capillary density was expressed as capillaries/mm^2.

Tissue Inflammatory Cell Quantification

Single-cell suspensions were prepared from muscle, BM, spleen, and whole blood. Anterior and posterior compartment hindlimb muscles were harvested, minced, and enzymatically dissociated in Hank's balanced salt solution (Invitrogen, Life Technologies, Grand Island, NY) supplemented with 1500 U/mL collagenase II (Invitrogen), 4.0 U/mL dispase (Invitrogen), and 2.5 mmol/L $CaCl_2$ (Sigma-Aldrich, St. Louis, MO) at 37°C for 90 minutes and filtered through a 40-μm strainer (BD Bioscience, San Jose, CA) to obtain a single-cell suspension. BM cells were obtained by flushing the femur with Hank's balanced salt solution containing 2% fetal bovine serum using a 25-gauge needle followed by treatment with red blood cell lysis buffer. A single-cell suspension of spleen cells was prepared by passing minced spleen through a cell strainer (Falcon; Becton Dickinson, Franklin Lakes, NJ) followed by treatment with red blood cell lysis buffer. Approximately 1 mL of blood was obtained in a heparinized syringe from isoflurane-anesthetized mice via cardiac puncture, placed into a 1.3-mL EDTA KE 1.3 micro tube (Sarstedt, Newton, NC), transferred to a fluorescence-activated cell sorting tube (BD Bioscience) and mixed with an equal volume of 2% dextran to sediment red blood cells for 30 minutes followed by treatment with red cell lysis buffer (Sigma-Aldrich). All single-cell suspensions were counted with a hemocytometer in the presence of trypan blue to obtain total cell counts and maintained on ice until use.

Single-cell suspensions were treated with monoclonal antibody 2.4G2 (BD Bioscience) for 20 minutes on ice to block Fc II/III receptors followed by incubation with conjugated antibodies at 4°C for 30 minutes. Anti−CD90-FITC (53-2.1), anti−B220-FITC (RA3-6B2), anti−CD49b-FITC (DX5), anti−NK1.1-FITC (PK136), anti−Ly6G-PE (1A8), anti−Ly6G-FITC (1A8), anti−CD11b-V450 (M1/70), anti−CD11c-PE (HL3), anti−I-Ab-PE (AF6-120.1), and anti−Ly6C-APC (AL-21) were purchased from BD Biosciences; anti−F4/80-PE (BM8) was purchased from eBioscience (San Jose, CA); anti−Ly6B.2-AF700 (7/4), anti−CD206-AF488 (MR5D3), and anti−CD301 (ER-MP23) were purchased from AbD Serotec (Raleigh, NC). Isotype controls were used to titrate each antibody to minimize background staining, 1 μg/mL propidium iodide (Sigma-Aldrich) was used for dead cell exclusion, and fluorescence-minus-one controls were used to generate gates.[43]

Monocytes were identified as CD11b$^+$(CD90/B220/CD49b/NK1.1/Ly6G)^{lo}(F4/80/I-Ab/CD11c)^{lo}Ly6C$^{hi/lo}$ as used by Swirski et al[5] to exclude neutrophils, T cells, B cells, natural killer (NK) cells, and dendritic cells. Macrophages were identified as CD11b$^+$F4/80$^+$ cells and macrophage subsets were identified by Ly6C, CD206, and CD301. Monocyte and macrophage numbers were calculated as total cells multiplied by percent cells within the monocyte/macrophage gate.

Flow Sorting of Cells to Isolate Macrophage Subtypes

Total cells that were isolated from injured muscle 3 days after CTX were resuspended in fluorescence-activated cell sorting buffer (Hank's balanced salt solution, 0.5% bovine serum albumin, 2 mmol/L EDTA) with 10 μg/mL Brefeldin A (eBioscience) and 100 μg/mL cyclohexamide (Sigma-Aldrich) to inhibit cytokine secretion and production, respectively. For each replicate ($n = 5$), cells isolated from the injured muscle of six mice were pooled for the experiment. After Fc receptor blocking, cells were incubated with anti−CD11b-V450 on ice for 30 minutes followed by incubation with anti−rat-kappa microbeads (Miltenyi Biotec, Bergisch Gladbach, Germany). Cells were passed through a MACS LS column (Miltenyi Biotec), and the positive fraction (CD11b$^+$) was collected, washed, and incubated with anti−F4/80-PE, anti−CD301-AF488, and anti−Ly6C-APC. The CD11b$^+$ cells were sorted on a FACSAria flow cytometer (Becton Dickinson) to collect CD11b$^+$F4/80$^+$Ly6C$^+$CD301$^-$ and CD11b$^+$F4/80$^+$Ly6C$^-$CD301$^-$ macrophage cell populations. A sample of the sorted macrophages was reanalyzed by flow cytometry; purity of the sorted groups ranged from 86% to 97%. The sorted cells were lysed in lysate buffer (100 μL of lysate buffer per million cells).[44]

Intracellular Cytokine Quantification and Arginase Activity Assay

Sorted CD11b$^+$F4/80$^+$Ly6C$^+$CD301$^-$ and CD11b$^+$F4/80$^+$Ly6C$^-$CD301$^-$ cell populations in lysate buffer were

submitted for cytokine/chemokine concentration determination in the mouse MAP panel B, a Luminex-based multiplex platform (Rules-Based Medicine, Austin, TX); the analytes measured included fibroblast growth factor-9 (FGF-9), granulocyte-macrophage colony-stimulating factor (GM-CSF), growth-regulated α protein (KC/GRO), interferon-γ (IFN-γ), IP-10, IL-1α, IL-2, IL-3, IL-4, IL-6, IL-7, IL-10, IL-11, IL-12p70, IL-17A, lymphotactin, MIP-1β, MIP-2, MCP-1, MCP-3, MCP-5, oncostatin-M (OSM), stem cell factor (SCF), T-cell−specific protein RANTES (RANTES), tissue inhibitor of metalloproteinases-1 (TIMP-1), TNF-α, and VEGF.

Arginase enzyme activity was determined in sorted $CD11b^+F4/80^+Ly6C^+CD301^-$ and $CD11b^+F4/80^+Ly6C^-CD301^-$ cell populations in lysate buffer at zeroth-order kinetics to provide a measure of arginase enzyme concentrations.[45] Cell lysates, in the presence of excess 100 mmol/L $MnCl_2$ (Sigma-Aldrich), were incubated at 56°C for 6 minutes to activate the arginase enzyme. The substrate, 0.5 mol/L arginine (Sigma-Aldrich), was added and incubated at 37°C for 2 hours to allow for the enzymatic conversion of arginine to urea. Urea standards (Sigma-Aldrich) were created. An acid mixture consisting of 1:3:7 $H_3PO_4/H_2SO_4/H_2O$ (EMD Millipore, Billerica, MA) was added to urea standards and samples to stop the reaction. An indicator, 6% α-isonitrosopropiophenone (α-ISPP; Sigma-Aldrich), was added to standards and samples, and incubated at 95°C for 30 minutes, followed by a 4°C incubation for an additional 30 minutes. Samples and standards were read at 540 nm on a microplate spectrophotometer.

Arginase activity was derived from the urea amount in each sample by the equation:

$$(\text{micrograms of urea}/\text{molecular weight of urea}) \times (\text{dilution factor}/\text{time in minutes of arginine incubation}).$$

Data were reported as units of arginase or more specifically as a unit of arginase activity equals the amount of enzyme required to hydrolyze 1 mmol/L of arginine per minute.

Data Analysis

We contrasted DTm- and DT-treated animals with regard to mean cross-sectional area at different time points using 2-way analysis of variance with a Bonferroni correction and a Tukey correction for pairwise comparisons by time within the DT group. Corresponding treatment group contrasts with regard to fat, injury, and necrosis were performed with Wilcoxon tests and Bonferroni corrections for multiple comparisons.

Flow cytometry data were analyzed with a quadratic model. We modeled the mean response of $\log_{10}$(total cells, monocytes and monocyte subsets, macrophages and macrophage subsets, neutrophils) with a quadratic model in terms of method (DT, DTm), day (2, 3, 4, 5, 6), method × day, day^2, and method × day^2, and contrasted mean responses by day with a Bonferroni correction. The method contrasts were to determine the significance of differences between DT- and DTm-treated animals.

Arginase activity and cytokine data was log transformed, and the two groups of $Ly6C^+CD301^-$ and $Ly6C^-CD301^-$ macrophages were analyzed using a two-tailed, paired *t*-test.

SAS version 9.2 for Windows (SAS Institute, Cary, NC) was used for statistical analysis, and all statistical testing was two-sided with an experiment-wise significance level of 5%. Interactions were tested at the 10% level of significance. Data were presented as means ± SEM.

Results

Ablation of CD11b Cells by a Single Dose of DT at Different Time Points Has Differential Effects on Skeletal Muscle Regeneration in CD11b-DTR Mice

We transiently ablated CD11b cells at different time points using CD11b-DTR mice to determine essential periods for monocyte/macrophage recruitment that were critical for muscle regeneration (Figure 1A). TA injury was assessed at day 7 after CTX injection. Residual necrosis, regenerated myofiber cross-sectional area, and fat area are quantitative phenotypes for muscle regeneration and indirect measures of macrophage function. Although the muscle injury in the TA was similar in all six groups (range, 86% to 95%), the residual necrosis (Figure 1B) greatly varied depending on the timing of the DT administration. DTm-injected control mice exhibited <3% residual necrosis at day 7 after CTX injury. However, mice that received a DT injection at days −0.5, 0, 1, or 2 exhibited progressively increasing residual necrosis, peaking at days 1 and 2. Interestingly, late DT administration (day 4) had similar residual necrosis as DTm controls. Cross-sectional area of regenerated fibers (Figure 1C) and the fat area (Figure 1D) were also affected by the timing of DT administration. Mice injected with DT at day 1 exhibited the smallest fiber size, whereas mice injected on day 0 had the highest intermuscular fat.

Early DT (Day 1) Treatment of CD11b-DTR Mice Impaired Skeletal Muscle Regeneration

Macrophages have been implicated in muscle fiber maturation and the resolution of inflammation at later stages of regeneration,[2] and this may not be measured at the day 7 time point used to screen the timing of DT administration. Therefore, DT administration at day 1 (early) or day 4 (late) was used to study skeletal muscle regeneration in the CTX model (Figure 2A). Day 0 (no injury) muscle had a mature fiber size of 2687 ± 101 μm^2, and intermuscular fat was not detected. For all groups, cross-sectional area was decreased ($P < 0.001$) and fat area was increased ($P \leq 0.003$) compared to day 0 at all post-injury time points. Early macrophage ablation (day 1 DT) resulted in smaller

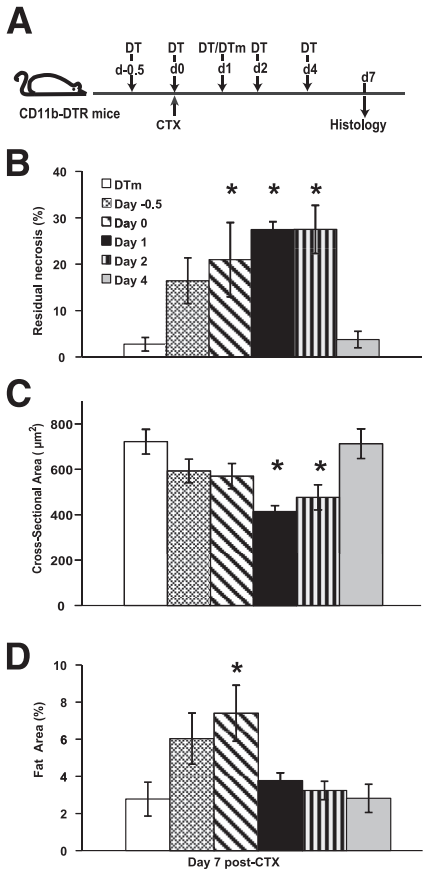

Figure 1 Time-dependent consequences of CD11b cell depletion in skeletal muscle regeneration. TA muscle regeneration was studied in CD11b-DTR mice and analyzed 7 days after CTX-induced injury. Timing of DT [day −0.5 (d−0.5) to day 4 (d4)] or control DTm (day 1) administration was in reference to CTX injection (**A**). Although the area of muscle injury was similar in the six groups (average of 86% to 95%), residual necrosis (**B**), cross-sectional area of regenerated myofibers (**C**), and fat area (%) (**D**) at day 7 after CTX were dependent on the timing of DT administration. Data are presented as means ± SEM. $n = 7$ to 10 mice/group. $^*P \leq 0.04$ versus mice treated with DTm at day 1 after injury (**B**–**D**).

regenerated myofiber size (Figure 2B) compared to the DTm control ($P < 0.001$). Although percent fat (Figure 2C) was similar at day 7 in all three groups, percent fat remained elevated with early ablation but decreased in the DTm control ($P \leq 0.003$). By contrast, late ablation (day 4 DT) exhibited similar regenerated myofiber size and fat accumulation as the DTm control group. Capillary density, expressed as capillaries/mm^2 (Figure 2D), was increased at day 21 ($P < 0.001$) compared to baseline (no injury, day 0) in all three groups. Furthermore, early (day 1) ablation resulted in increased ($P = 0.002$) capillary density compared to the DTm control. Finally, capillaries/fiber (Figure 2E) in all the groups were similar to baseline (no injury, day 0).

Representative images of early macrophage ablation group (day 1 DT) and control group are shown in Figure 3. Normal myofibers (Figure 3C) have a uniform size and a polygonal shape with peripheral nuclei. Following injury, there was a vigorous mononuclear cell infiltrate in DTm control mice at day 2 after injury (Figure 3A) that increased by day 3. By contrast, CD11b-DTR mice receiving DT early (day 1) exhibited minimal mononuclear cell accumulation at days 2 and 3 (Figure 3B) with increased neutrophils compared to DTm control mice. By day 7 after injury, DTm control mice had small, regenerating muscle fibers with minimal necrosis (Figure 3D), whereas early DT-treated mice had extensive necrotic muscle fibers (Figure 3E). Early DT-treated mice (Figure 3H) had smaller myofibers with more prevalent adipocytes than DTm control mice at 21 days after injury (Figure 3G). Of note, late DT-treated (day 4) mice showed a similar phenotype compared to DTm control mice at day 7 and day 21, respectively (Figure 3, D and F, and G and I, respectively).

Early DT Treatment of CD11b-DTR Mice Exhibited Diverse Effects on Total Cells and Monocytes in BM, Blood, and Spleen

Given the impairments in muscle regeneration with early DT treatment (Figures 2 and 3), flow cytometry was used to determine the expression pattern of monocytes, defined as CD11b$^+$(CD90/B220/CD49b/NK1.1/Ly6G)^{lo}(F4/80/I-Ab/CD11c)^{lo}Ly6C$^{hi/lo}$ cells,[5] in BM, blood, and spleen in controls (DTm) and following ablation with DT treatment at day 1 after CTX injection. Day 0 (no injury) and day 1 after CTX were used to establish monocyte patterns before ablation and did not receive DT or DTm. Days 2 to 6 after CTX injury were used to determine the effect of day 1 DT on monocyte numbers compared to the DTm control (Figure 4A). With early DT treatment, total cells (Figure 4B) in BM were similar to controls (DTm) except for a decrease ($P \leq 0.007$) at days 2 to 3 and an increase ($P < 0.001$) at day 6, suggesting that cell ablation occurred at days 2 to 3, leading to a rebound in BM total cells at day 6. Interestingly, BM monocytes (Figure 4E) in mice receiving DT were similar to controls at days 2 to 3, suggesting that monocyte ablation in the BM did not occur, but monocytes still increased ($P < 0.001$) in mice receiving DT compared to controls at days 4 and 6. The distribution of Ly6C^{hi} (proinflammatory) and Ly6C^{lo} (anti-inflammatory) monocytes[5] in BM (Figure 4H) revealed similar numbers of both subtypes of monocytes in DTm control mice. With early DT treatment, Ly6C^{hi} monocytes were increased ($P = 0.003$) at day 6, whereas Ly6C^{lo} monocytes were increased ($P \leq 0.03$) at days 4 and 6 compared to controls.

In blood, total cells (Figure 4C) decreased ($P < 0.001$) at day 2 with early DT treatment but were similar to DTm control groups at all other time points. Blood monocytes (Figure 4F) were similar to day 0 throughout the time course of injury in control mice, with decreased ($P < 0.001$) monocytes in DT-treated mice at day 2 compared to controls. The distribution of Ly6C^{hi} and Ly6C^{lo} monocytes (Figure 4I) was similar in control mice throughout the injury time course. With ablation, there were decreases ($P < 0.001$) compared to controls in both Ly6C^{hi} and Ly6C^{lo} monocytes at day 2.

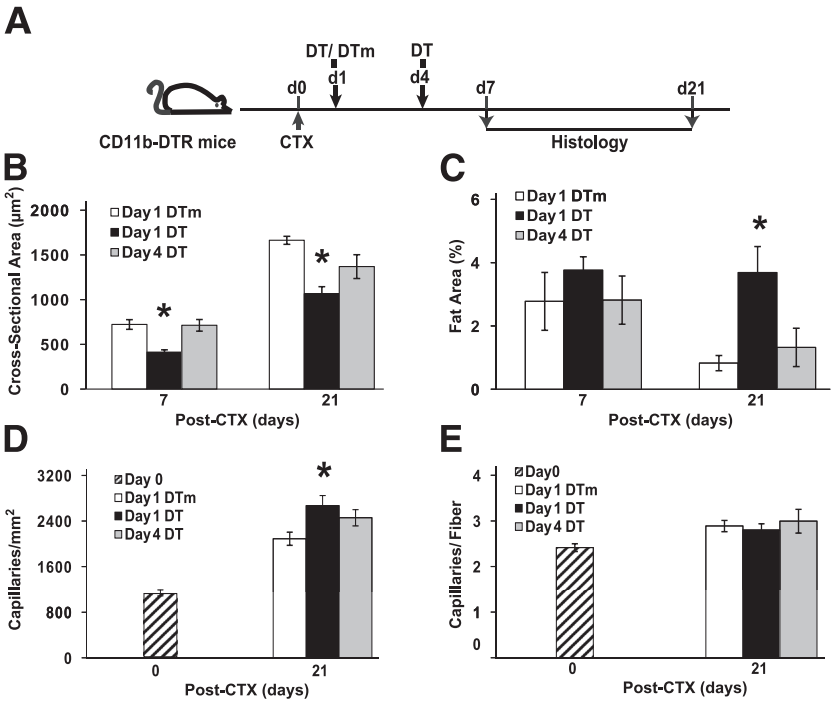

Figure 2 Impaired muscle regeneration with early (day 1) DT administration compared to control DTm and late (day 4) DT. TA muscle injury was induced in CD11b-DTR mice and analyzed after CTX-induced injury. Timing of DT or DTm administration was relative to CTX injection (**A**). Regenerated myofiber cross-sectional area (**B**), fat area (%) (**C**), capillaries/mm^2 (**D**), and capillaries/fiber (**E**) measurements were performed in the TA muscle at day 0 (no injury) and after CTX-induced injury at indicated time points. Myofiber size at day 0 (no injury) was 2687 ± 101 mm^2, and intermuscular fat was not detected in uninjured muscle. Data are presented as means ± SEM. $n = 7$ to 11 mice/group/time point. *$P \leq 0.003$ versus mice treated with DTm at day 1 (**B**–**D**).

Although DT ablated total cells in the blood at day 2 ($P < 0.001$), only a portion of the ablated cells were monocytes, and the recovery of blood monocytes was accomplished with predominately Ly6C^{hi} cells.

In the spleen, total cells (Figure 4D) were similar in controls and DT-ablated mice. However, splenic monocytes (Figure 4G) increased ($P \leq 0.01$) at days 5 and 6 after injury in early DT-treated mice compared to controls. The distribution of Ly6C^{hi} and Ly6C^{lo} monocytes (Figure 4J) revealed similar numbers of both subtypes of monocytes in DTm control mice. The increased ($P < 0.001$) monocytes at days 5 and 6 resulted predominately from elevations in the Ly6C^{hi} population.

Effects of Early DT Treatment of CD11b-DTR Mice on Muscle Inflammatory Cells

Given the impairment in muscle regeneration with early DT treatment (day 1) in CD11b-DTR mice, we performed flow cytometry to quantify inflammatory cells in injured muscle (Figure 5, Supplemental Table S1, and the gating strategy shown in Supplemental Figure S1). Total cells in skeletal muscle (Figure 5B) decreased ($P = 0.006$) only at day 3 but increased ($P = 0.001$) at day 5 with DT treatment compared to the DTm control. Neutrophils, defined as CD11b$^+$Ly6G$^+$ cells (Figure 5C), peaked at days 1 to 2 and rapidly decreased thereafter in control mice compared to day 0. By contrast, DT treatment resulted in increased ($P \leq 0.02$) neutrophils at days 3 to 6 compared to the DTm control.

Monocytes (Figure 5, D, F, and H) and macrophages (Figure 5, E, G, and I, and Supplemental Table S1) exhibited interesting expression patterns in injured muscle. In the controls relative to day 0, monocytes (Figure 5D) immediately increased and peaked at day 1 and gradually decreased. Ly6C$^+$ monocytes predominated at days 1 to 2, and Ly6C$^-$ monocytes were increased at day 1 and remained at a similar level through day 4. By contrast, early DT treatment resulted in an exaggerated increase ($P \leq 0.04$) in monocytes at days 4 and 5 compared to the control groups. The distribution of Ly6C$^+$, but not Ly6C$^-$, monocytes (Figure 5, F and H) was affected by early DT treatment, with exaggerated increases ($P \leq 0.02$) occurring in Ly6C$^+$ monocytes at days 4 and 5 after injury compared to control mice.

In contrast to the sustained elevation of monocytes in injured muscle, macrophages, defined as CD11b$^+$F4/80$^+$ cells (Figure 5E and Supplemental Table S1), increased after injury, with peak numbers occurring at day 4 in the control mice. Early DT resulted in decreased ($P \leq 0.03$) macrophages at days 2, 3, and 4 compared to controls, leading to delayed and reduced macrophages. Although macrophages after day 4 were similar in DT and control groups, no distinct peak was observed in DT-treated animals. To further characterize macrophage subsets, we used Ly6C, CD206, and CD301 for further phenotypic analysis of the CD11b$^+$F4/80$^+$ cell populations (Supplemental Figure S1). CD206 and CD301 were coexpressed on macrophages and exhibited similar results when combined with Ly6C (data not shown), CD301 expression data are shown (Figure 5, G and I). The main macrophage subsets in both the control group and early ablation group were Ly6C$^+$ cells or Ly6C$^-$CD301$^-$ double-negative cells. There was minimal CD301 expression among all groups. In the control group following injury (Figure 5, G and I), the Ly6C$^+$CD301$^-$ macrophage subset predominated at days 1 to 3 and was minimal by day 6. By

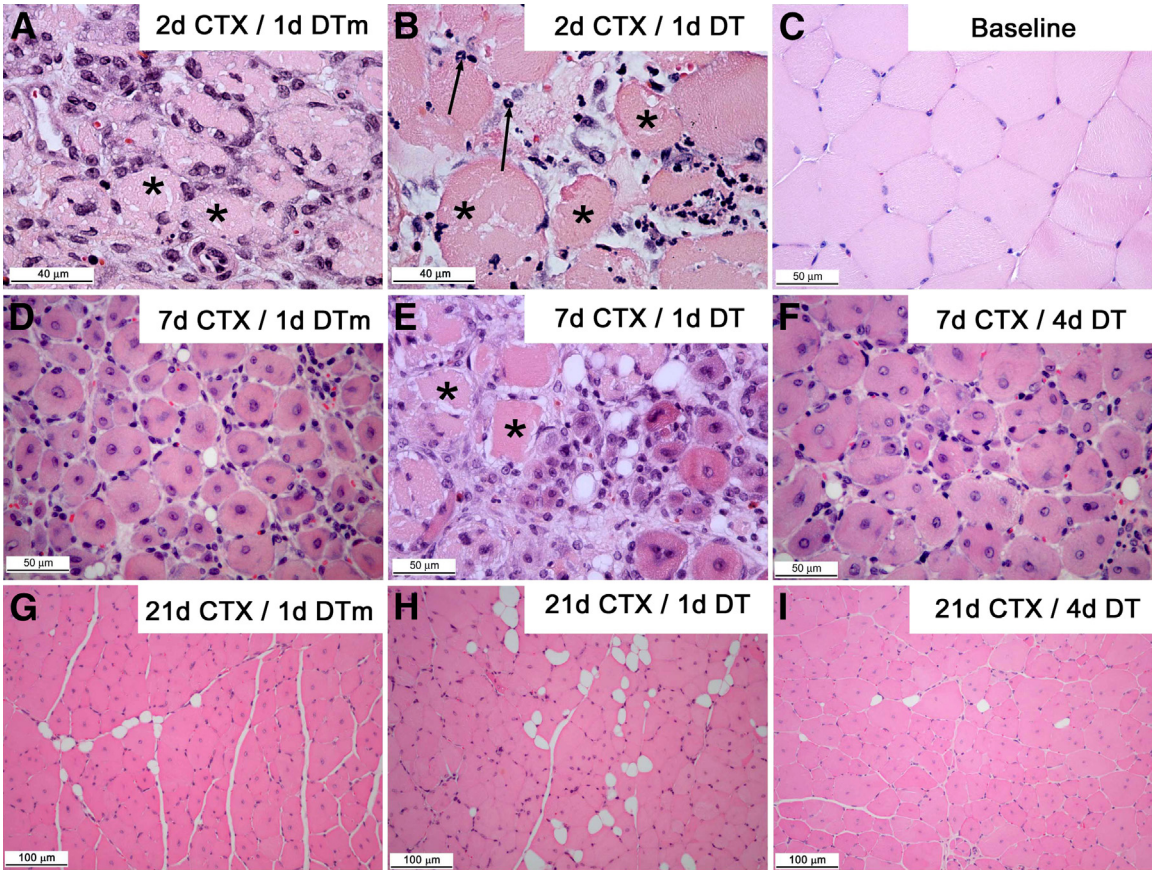

Figure 3 Inflammation, myofiber necrosis, and tissue regeneration in TA muscle following CTX-induced injury in CD11b-DTR mice after administration of DT or DTm control. Images were derived from TA muscle of CD11b-DTR mice. Control mice received DTm (**A**, **D**, and **G**) and were sacrificed at the indicated time point after CTX injection [day 2 (2d), 7, or 21 CTX]. DT was administered at day 1 after CTX (**B**, **E**, and **H**) or day 4 after CTX (**F** and **I**). Thus, specimens were derived at day 0 (no injury, baseline) (**C**), 2 (**A** and **B**), 7 (**D**–**F**), or 21 (**G**–**I**) days after CTX-injury. **Asterisks** identify necrotic muscle fibers; **arrows** indicate neutrophils, paraffin sections (3–4 μm), hematoxylin and eosin stain.

contrast, the double-negative ($Ly6C^{-}CD301^{-}$) macrophage subset was the main cell population at days 3 to 6 with a peak at day 4 and a sustained presence at days 5 and 6. Early CD11b-positive cell ablation drastically reduced ($P < 0.001$) the $Ly6C^{+}CD301^{-}$ macrophage subset at day 2, resulting in a delayed accumulation of $Ly6C^{+}CD301^{-}$ compared to controls, thus DT treatment shifted, but did not decrease, $Ly6C^{+}CD301^{-}$ macrophage accumulation. In parallel, the $Ly6C^{-}CD301^{-}$ macrophages were decreased ($P \leq 0.02$) at days 2, 3, and 4 compared to controls, and became the predominant cell population at days 5 and 6. Although DT treatment shifted the accumulation of both $Ly6C^{+}CD301^{-}$ and $Ly6C^{-}CD301^{-}$ macrophages, the double-negative ($Ly6C^{-}CD301^{-}$) macrophage population demonstrated an overall decreased accumulation in DT-treated mice, never reaching the peak levels observed in control mice.

Characterization of $CD11b^{+}F4/80^{+}$ Macrophage Subsets in Muscle

To further characterize the $Ly6C^{+}CD301^{-}$ and the double-negative ($Ly6C^{-}CD301^{-}$) population, cytokine expression in sorted cells was determined. Many cytokines and chemokines associated with M1 macrophages (IL-1α,[46,47] MCP-1[48–51], MCP-3,[50,51] MIP-2,[3] OSM,[52] TNFα,[7,47,49,53] and VEGF[5,54]) exhibited increased ($P \leq 0.05$) expression in the $Ly6C^{+}CD301^{-}$ macrophage population relative to the double-negative population (Figure 6, B, D–G, I, and J). Other cytokines that have not previously been associated with the M1 population (FGF-9, lymphotactin, and SCF) were also increased ($P \leq 0.04$) in the $Ly6C^{+}CD301^{-}$ population relative to the double-negative population (Figure 6, A, C, and H). Additionally, arginase activity (Figure 6K) was higher in the double-negative population ($P = 0.02$) than in the $Ly6C^{+}CD301^{-}$ macrophages.

Discussion

The present study investigated monocyte/macrophage subsets in skeletal muscle regeneration by transiently ablating monocytes/macrophages at different time points after injury in CD11b-DTR mice. Early monocyte/macrophage ablation by a single DT treatment altered the phenotypic switch of macrophage subsets and impaired muscle regeneration. However, late monocyte/macrophage ablation had minimal

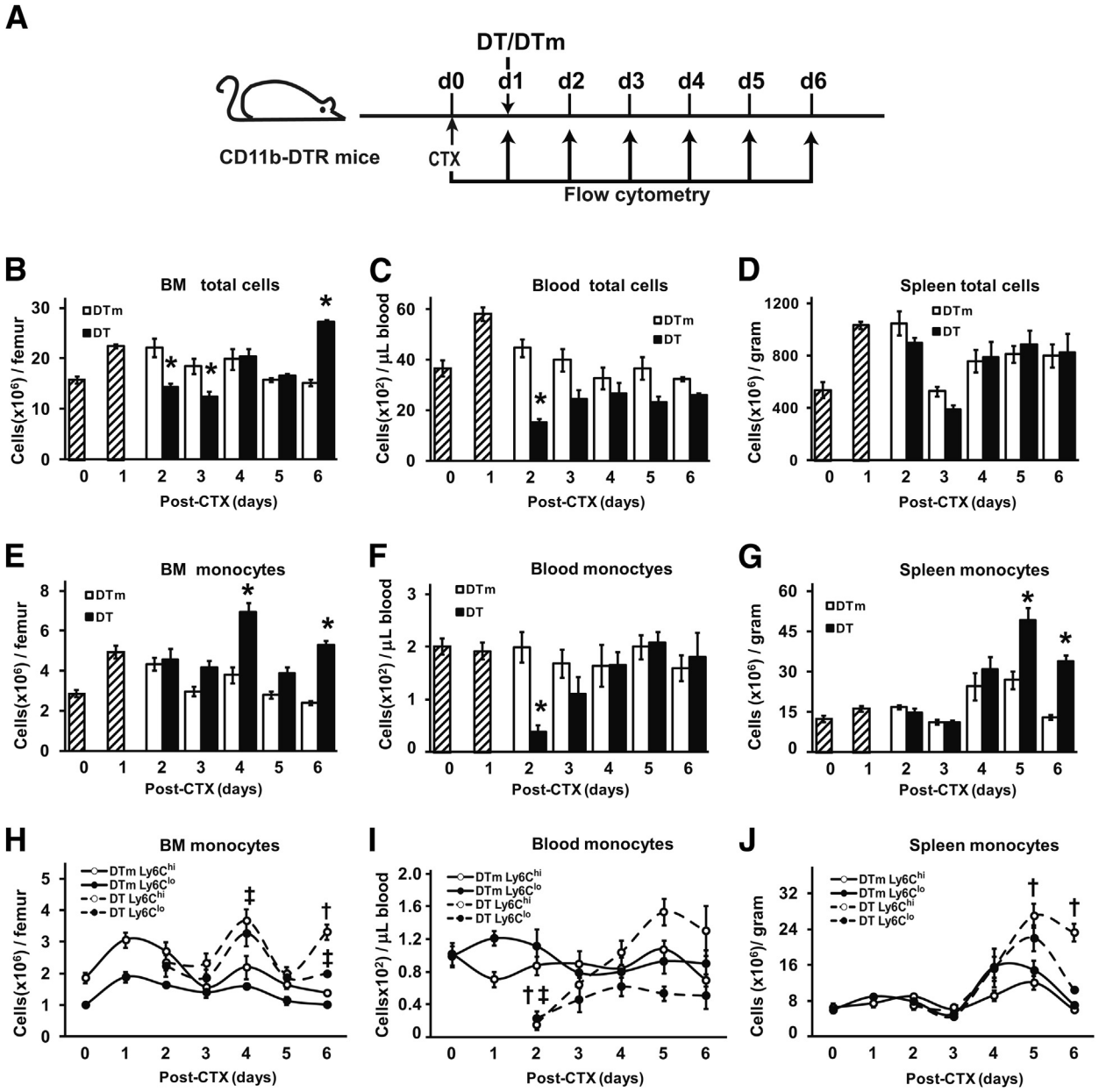

Figure 4 Diverse effects of early DT treatment on total cells and monocytes in BM, blood, and spleen. Timeline of CTX and DT/DTm injections and flow cytometry (**A**). Hatched bars (**B**–**G**) are cell counts per gram of tissue from uninjured (day 0) and injured (day 1) mice that did not receive DT or DTm (control) injections. BM (**B**, **E**, and **H**), blood (**C**, **F**, and **I**), and spleen (**D**, **G**, and **J**) were collected for flow cytometry analysis. Results are provided as total cells (**B**–**D**), monocytes ($CD11b^{+}(CD90/B220/CD49b/NK1.1/Ly6G)^{lo}(F4/80/I\text{-}Ab/CD11c)^{lo}Ly6C^{hi/lo}$) (**E**–**G**), and monocyte subsets ($Ly6C^{hi}$ or $Ly6C^{lo}$) (**H**–**J**). Data are means ± SEM. $n = 4$ to 6 mice/group/time point. $^{*}P \leq 0.01$ versus DTm controls at each corresponding time point (**B**, **C**, and **E**–**G**); $^{\dagger}P \leq 0.003$ $Ly6C^{hi}$ monocytes in DT- versus DTm-treated animals at each corresponding time point (**H**–**J**); and $^{\ddagger}P \leq 0.03$ $Ly6C^{lo}$ monocytes in DT- versus DTm-treated animals at each corresponding time point (**H** and **I**).

effect on skeletal muscle regeneration. Our results suggest that the ratio of $Ly6C^{+}$ and $Ly6C^{-}$ macrophages, and their temporal expression, is critical in muscle regeneration.

Macrophages play a critical role during healing/regeneration processes,[1,7,55] both in removing necrotic tissue and promoting repair.[8,56] In muscle, $Ly6C^{+}$ monocytes/macrophages predominated at early time points after injury and exhibited a proinflammatory profile, whereas $Ly6C^{-}$ monocytes/macrophages were the main cell population with an anti-inflammatory profile at later stages of regeneration.[7,55] However, both of these studies quantified the combination of monocytes and macrophages rather than dividing monocytes and macrophages into distinct groups. CD11b-DTR transgenic mice have been widely used for monocyte/macrophage ablation.[7,15,35,36,57–59] DT-induced ablation, demonstrated by our data and previous reports,[7,41] is effective for approximately 2 days. We transiently ablated various monocyte/macrophage populations by treating CD11b-DTR

mice with a single dose of DT at different time points to investigate the kinetics of Ly6C$^+$ and Ly6C$^-$ monocytes as well as macrophages in skeletal muscle regeneration. We used day 7 after injury to determine the effect of monocyte/macrophage ablation at various time points for differences in residual necrosis, fat accumulation, and regenerated fiber size. Although DT treatment on CD11b-DTR mice at days 0, 1, and 2 resulted in increased residual necrosis at day 7, only

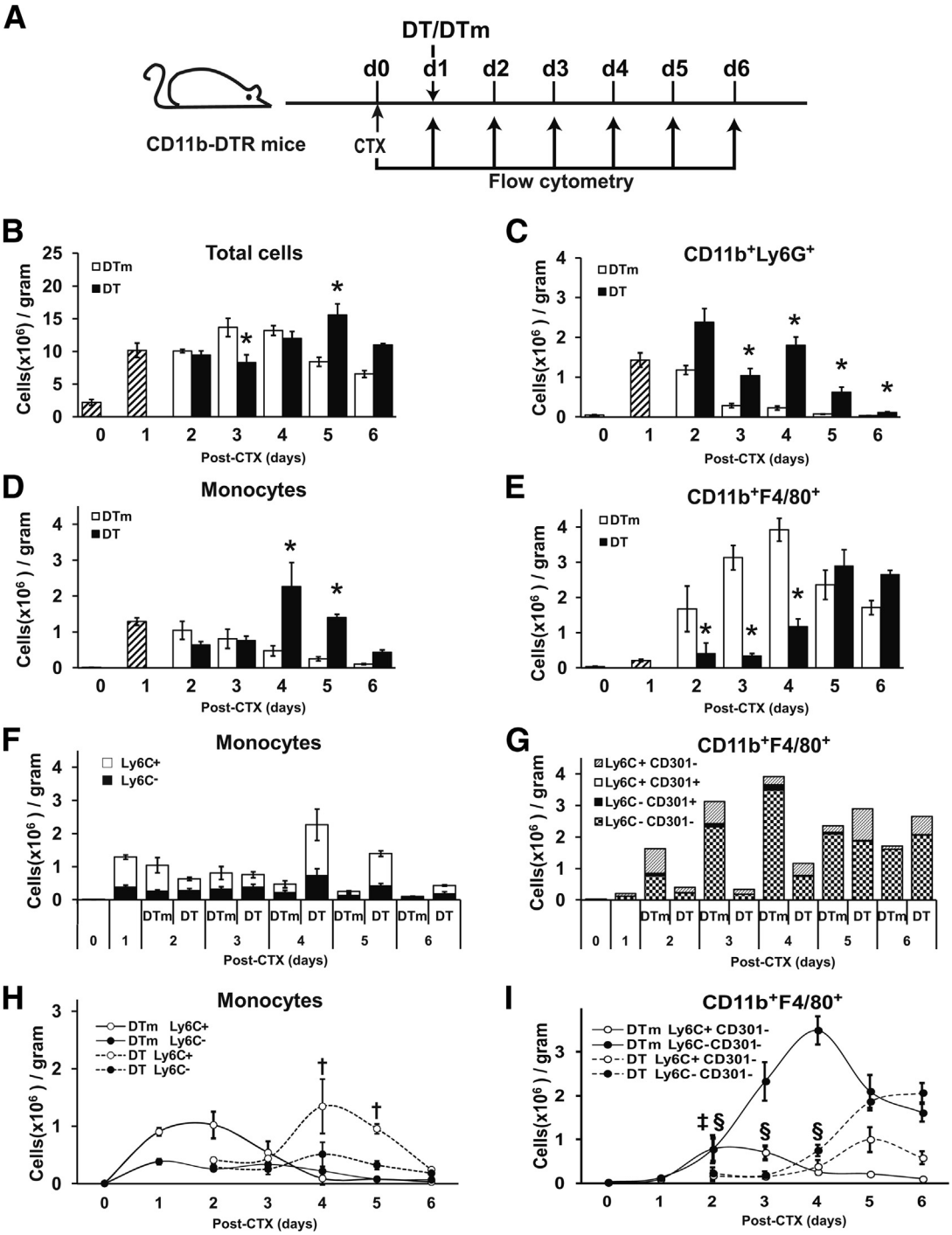

Figure 5 Effect of ablation on accumulation of inflammatory cells in injured muscle. Muscle was injured with CTX on day 0 in CD11b-DTR mice followed by DTm or DT treatment on day 1. Inflammatory cells were analyzed by flow cytometry at day 0 (no injury) and each day after CTX injury (**A**). Hatched bars (**B**–**E**) and the first two data sets in (**F** and **G**) are cell counts per gram of tissue from uninjured (day 0) and injured (day 1) mice that did not receive DT or DTm (control) injections. Results are provided as total cells (**B**), neutrophils (CD11b$^+$/Ly6G$^+$) (**C**), monocytes (CD11b$^+$(CD90/B220/CD49/NK1.1/Ly6G)$^-$(F4/80/I-Ab/CD11c)$^-$Ly6C$^{+/-}$) (**D**), monocyte subsets (**F** and **H**), macrophages (CD11b$^+$F4/80$^+$) (**E**), and macrophage subsets (**G** and **I**). Data are presented as means ± SEM. n = 4 to 6 mice/group/time point. *$P \leq 0.04$ versus DTm animals at each corresponding time point (**B**–**E**); $^{\dagger}P \leq 0.02$ Ly6C$^+$ monocytes versus DTm animals at each corresponding time point (**H**); $^{\ddagger}P < 0.001$ Ly6C$^+$CD301$^-$ macrophages versus DTm animals at each corresponding time point; and $^{\S}P \leq 0.02$ Ly6C$^-$CD301$^-$ macrophages versus DTm animals at each corresponding time point (**I**).

mice with DT treatment at days 1 and 2 exhibited smaller regenerated fibers. Interestingly, mice with DT treatment at day 0 showed an increase in fat accumulation (Figure 1), suggesting that the microenvironment in injured muscle at day 0 may have an effect on the proliferation and differentiation of adipogenic progenitor cells in muscle, whereas the monocyte/macrophage-induced microenvironment at day 1 preferentially affected myogenic progenitor cells. Nevertheless, although fat accumulation was similar in early ablation, compared to late ablation and controls at day 7, fat accumulation remained elevated at day 21 after early ablation, whereas it decreased in late ablation and control groups (Figure 2C), suggesting that events regulated by monocytes/macrophages at early time points alter the long-term course of fat accumulation.

Increased fat accumulation in muscle, in association with decreased macrophages recruitment, has also been observed in *Ccr2*$^{-/-}$ mice in several different muscle injury models,[20,22,60], and increased fat accumulation maybe an indicator of abnormal/altered muscle regeneration. Two studies demonstrated that accumulated adipocytes originated from fibrocyte/adiopocytes progenitors (FAP) that reside in skeletal muscle[61,62] rather than from myogenic progenitor cells. FAP enhance proliferation and differentiation of myogenic progenitors but do not generate myofibers. During homeostasis and regeneration, FAP remain in an undifferentiated state due to inhibition signals from muscle lineage cells. After muscle injury, FAP differentiate into adipocytes and fibroblasts, which may inhibit the activation of muscle progenitor cells. Altogether, increased fat accumulation in skeletal muscle maybe due to FAP differentiation into adipocytes secondary to the absence of signals provided by the early infiltrating monocytes/macrophages.

In addition to muscle regeneration, macrophages are also important in angiogenesis, which is essential for establishing capillary networks necessary for muscle regeneration.[63,64] Our previous work demonstrated maximal capillary density (capillaries/mm^2) was present at day 7 after injury in C57BL/6J mice and decreased thereafter, returning to baseline levels by day 28.[22] In this study, we measured angiogenesis using capillary density at days 0 and 21. Angiogenesis could not be quantified at day 7 after injury in CD11b-DTR mice because of extensive residual necrosis. Thus, the increased capillaries/mm^2 in the early ablation group at day 21 compared to day 0, which was not observed in the DTm control and late ablation groups at day 21, suggests that the return to baseline capillary density may have been delayed by early macrophage ablation (Figure 2). Alternatively, increased capillaries/mm^2 in the early ablation group at day 21 could have resulted from the delayed, but sustained, presence of Ly6C$^+$ macrophages (Figure 5, G and I), which is consistent with Willenborg et al[54] showing that Ly6C$^+$CD11b$^+$F4/80$^+$ macrophages were the main source of VEGF; a critical factor in initiating vascularization during wound healing.

In addition to the changes in fat accumulation and capillary density, early, but not late, ablation, resulted in a smaller regenerated fiber size compared to DTm controls, which is consistent with a previous study.[7] A possible explanation is that DT treatment only ablates circulating monocytes, but not monocytes/macrophages that were present in muscle at the time of DT administration. Further support for this possibility derives from Arnold et al's[7] intravenous injection of DT at day 4 after muscle injury that did not alter either F4/80$^+$ or CD11b$^+$ cells isolated from muscle. However, intramuscular injection of DT at day 5 resulted in decreased F4/80$^+$ cells with a twofold increase in CD45$^+$ cells at day 6 versus PBS-injected muscle, suggesting that intramuscular injection of DT induced a secondary inflammatory response in muscle that consisted of cells other than macrophages. Taken together, these data support the notion that the intramuscular injection of DT is necessary to ablate macrophages that are already present in the muscle, whereas intraperitoneal and intravenous DT injection ablates circulating monocytes.

Given the differences in capillary density, regenerated fiber size, and fat accumulation with early ablation, detailed flow cytometry studies were performed to determine the kinetics of inflammatory cell recruitment in early-ablated mice and controls. Neutrophils are key players in early inflammation, but the continued presence of neutrophils can extend muscle injury and membrane damage.[65–67] Persistence of neutrophils in injured tissue may reflect a reduction in macrophage-mediated neutrophil clearance.[68,69] In this study, monocytes and macrophages were transiently ablated in skeletal muscle; however, CD11b$^+$Ly6G$^+$ neutrophils, a myeloid cell population that were also expected to be ablated in muscle, remained elevated in early DT-treated mice compared to control mice (Figure 5C), which is consistent with previous observations.[35,36] A possible explanation is that neutrophils have a lower density of CD11b compared to monocytes/macrophages, which may protect neutrophils from ablation in DTR mice.[15,41] Alternatively, DT administration may affect recruitment to injured muscle, but may not result in ablation of neutrophils that were already present in muscle at day 1 after injury. Further studies are needed to determine the potential mechanisms of the persistent elevations of neutrophils after early ablation.

To determine monocyte kinetics, we studied the effects of early ablation on monocytes in BM, blood, spleen, and muscle. In response to injury, monocytes are released from BM to blood, enter injured tissue, and differentiate into macrophages.[70,71] In addition to BM, the spleen has been identified as a reservoir for monocytes that exhibit a similar phenotype as blood monocytes.[5,71] In a myocardial infarction model, monocytes decreased in the spleen and increased in injured tissue. However, the number of monocytes in BM remained similar, suggesting that spleen was the primary reservoir, rather than BM, for monocytes mobilized to injured tissue.[5] By contrast, in control mice in the skeletal muscle injury model, monocytes in BM increased at days 1 to 2 after injury (Figure 4E), whereas monocytes in blood and spleen remained similar to day 0 after injury (Figure 4, F and

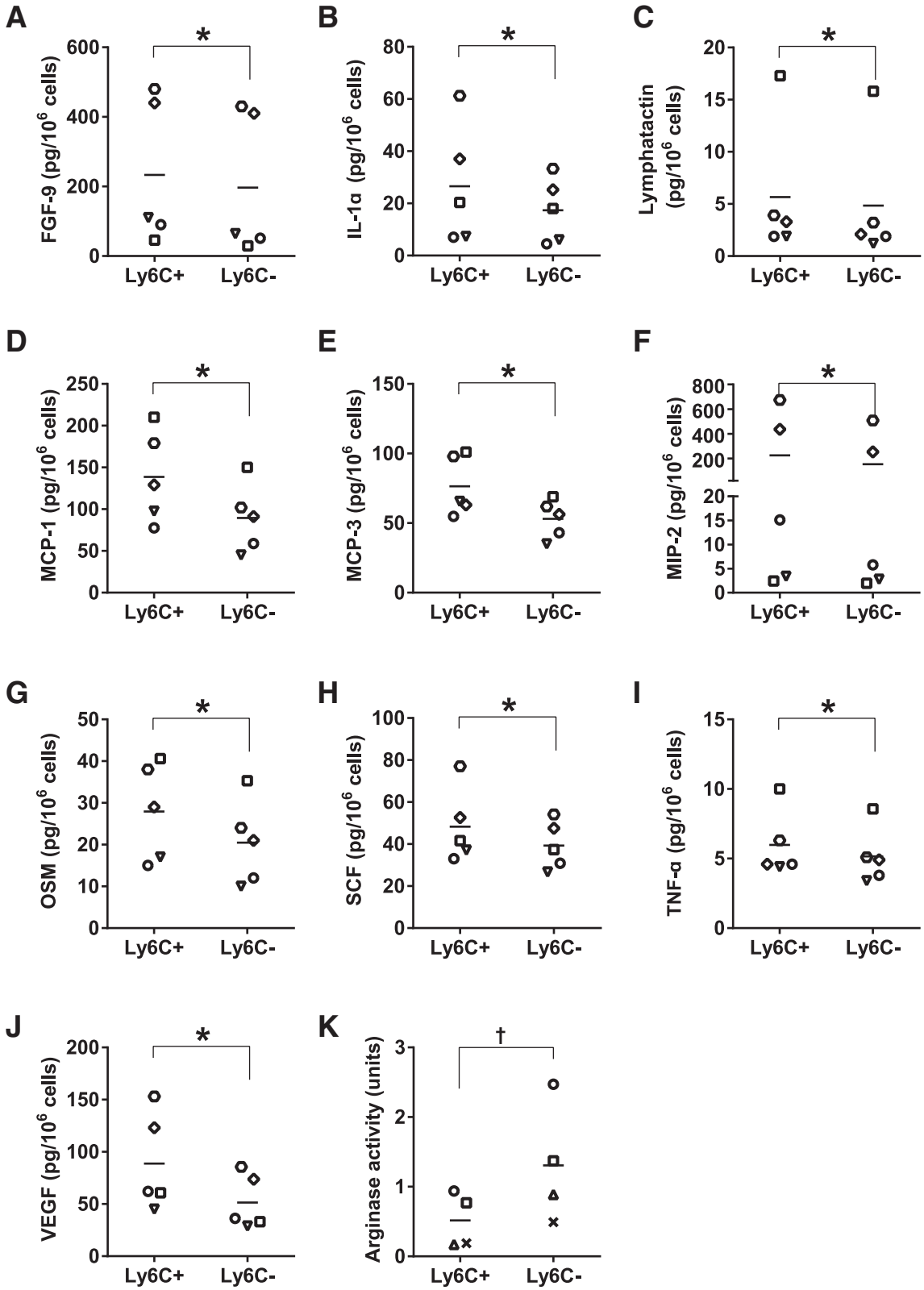

Figure 6 Characterization of $CD11b^+F4/80^+$ macrophage subsets. $Ly6C^+CD301^-$ and $Ly6C^-CD301^-$ macrophages ($CD11b^+F4/80^+$) were sorted from CTX-injured muscle at day 3. Sorted cells were lysed with lysate buffer, and the lysates were used for measuring the concentrations of cytokines (**A**–**J**) using a bead-based multiplexing immunoassay. Measured analytes that were not significantly different between the macrophage subsets or below the level of detection included GM-CSF, KC-GRO, IFNγ, IL-2, IL-3, IL-4, IL-6, IL-7, IL-10, IL-11, IL-12p70, IL-17A, IP-10, MCP-5, MIP-1β, RANTES, and TIMP-1. Lysates were also used to determine arginase activity (**K**). Data are presented as means ± SEM. $n = 4$ to 5; cells isolated from the skeletal muscles of six mice were pooled for each replicate. *$P \leq 0.05$ cytokines in $Ly6C^+CD301^-$ versus $Ly6C^-CD301^-$ cells (**A**–**I**), for arginase activity; †$P = 0.02$ $Ly6C^+CD301^-$ versus $Ly6C^-CD301^-$ cells (**K**).

G). These observations suggest that the monocyte elevations in muscle after injury (Figure 5D) may have emanated from the BM. Interesting patterns emerged with ablation; blood monocytes (Figure 4F) were ablated at day 2, but monocytes in BM and spleen were similar to controls at day 2. In fact, monocytes exhibited an exaggerated increase at day 4 in the BM, but at day 5 in the spleen, compared to control mice, suggesting that the precedent increase in BM monocytes may have been the source of the increase 1 day later in spleen. Although we used the same antigens to define monocytes as the cardiac ischemia model,[8] our results differed. Possible explanations for the differences in the two studies include cardiac versus skeletal muscle injury, as well as different mouse strains of C57Bl/6J versus FVB used.

Differences also existed in the monocyte kinetics in the BM and splenic compartments, the sequential expression/recruitment of $Ly6C^+$ and $Ly6C^-$ monocytes in injured muscle was different from the cardiac ischemia model.[8] In control mice, muscle total monocytes increased at day 1 and gradually decreased (Figure 5D). However, $Ly6C^+$ monocytes predominated at early stages (days 1 to 3), and $Ly6C^-$ monocytes were increased at day 1 and remained at a similar level through day 4. With ablation, $Ly6C^+$ monocytes showed a similar, but delayed, expression pattern compared to control mice, with increases in $Ly6C^+$ monocytes occurring at days 4 and 5 in muscle (Figure 5, F and H). Although these two monocyte populations appeared in tissue after injury in control mice, the mechanisms that control the $Ly6C^+/Ly6C^-$ monocyte ratio are injury and tissue dependent. In a myocardial infarct model, $Ly6C^{hi}$ and $Ly6C^{lo}$ subsets were sequentially recruited using different chemokine pathways, MCP-1 essential for $Ly6C^{hi}$ monocyte recruitment and CXC3CL1 essential for $Ly6C^{lo}$ recruitment.[5,8] A possible explanation in our model is that in the context of the microenvironment provided by early DT treatment, chemokines such as MCP-1 and CX3CL1 that are expressed in injured muscle may also have been altered, resulting in the recruitment of both $Ly6C^+$ and $Ly6C^-$ monocytes.

In addition to investigating the kinetics of monocyte subsets in injured muscle, we also explored the kinetics of macrophage subsets. To our knowledge, this is the first study that determined the kinetics of the well-characterized monocyte and macrophage subsets in muscle tissue and their roles in muscle regeneration after ablation. The study by Arnold et al[7] used *Cx3cr1*$^{gfp/+}$ mice, and after muscle injury, the initial $CX3CR1^{lo}Ly6C^+$ cells switched to the $CX3CR1^{hi}Ly6C^-$ population. Brechot et al[55] used F4/80 and Ly6C combinations. Both of these studies used surface markers that represented a mixed population of monocytes and macrophages. A third study focused on the kinetics of $CD45^+F4/80^+$ macrophages and their $Ly6C^+$ and $Ly6C^-$ subsets in muscle regeneration and did not determine monocyte kinetics.[72] We took advantage of selective and transient monocyte/macrophage ablation in CD11b-DTR mice, rather than achieving only partial ablation for an extended time after injury as used in previous macrophage depletion studies.[1,16–19] More importantly, as shown in Figure 5, G and I, early ablation resulted in a delayed $Ly6C^+CD11b^+F4/80^+$ macrophage accumulation in muscle, which was accompanied by a delayed and decreased accumulation of $Ly6C^-CD11b^+F4/80^+$ macrophages compared to control mice. Our study suggests that the timing and magnitude of $Ly6C^-CD11b^+F4/80^+$ macrophages is dependent on the duration and timing of the $Ly6C^+CD11b^+F4/80^+$ macrophages, and the disordered accumulation of macrophage subsets by early DT treatment impaired skeletal muscle regeneration; these results are consistent with a previous observation.[72]

Studying monocyte and macrophage populations in muscle regeneration, and the effect of early ablation, led to several interesting observations. Blood monocytes remained remarkably constant, with similar numbers at baseline and all post-injury time points, with roughly equal numbers of $Ly6C^{hi}$ and $Ly6C^{lo}$ monocytes. At day 1 after injury in muscle, monocytes (1×10^6 cells/g) predominated, and relatively few macrophages were present, with the numbers of monocytes gradually decreasing thereafter, suggesting that recruited monocytes differentiated into macrophages in tissue. By contrast, few macrophages were present at day 1, but rapidly increased to approximately 3 to 4×10^6 cells/g at days 3 and 4 and decreased to approximately 1.5×10^6 cells/g thereafter. Similar to monocytes, $Ly6C^+$ macrophages peaked at early time points, but the majority of macrophages at days 3 to 6 were $Ly6C^-$. Given the relative numbers of monocytes and macrophages within injured muscle, questions arise regarding monocyte-to-macrophage differentiation, as well as recruitment versus proliferation within the injured tissue. Macrophages can proliferate in tissues.[73] The relatively lower numbers of monocytes in injured muscle compared to macrophages, and the transient, but greater, magnitude increases in macrophages, suggest that macrophage proliferation occurred in muscle. However, the relative contributions of monocyte/macrophage recruitment versus proliferation remain to be determined.

With early ablation, monocytes decreased at day 2 in blood, but not in muscle, BM, or spleen. Of note, exaggerated increases in monocytes in muscle at days 4 to 5 and in spleen at days 5 and 6 may have derived from the increased monocytes in the BM at day 4. By contrast, muscle macrophages were decreased with early ablation at days 2 to 4, reaching levels of almost 3×10^6 cells/g at day 5, but never attaining the approximately 4×10^6 cells/g attained in control mice. Ablation resulted in a delay, but with similar numbers of $Ly6C^+$ macrophages compared to controls, however; $Ly6C^-$ macrophages remained decreased compared to controls, thereby leading to altered ratios of $Ly6C^+$ and $Ly6C^-$ macrophages with ablation that may have affected muscle regeneration. Interestingly, the exaggerated increase in muscle monocytes at days 4 and 5 in ablated animals did not result in macrophage levels being similar to control animals, suggesting that the increased monocytes could not compensate for the decreased

macrophages in ablated mice in regard to removing necrotic tissue and enhancing regenerated myofiber cross-sectional area (Figure 1). Thus, alterations in monocyte recruitment and reductions in the Ly6C$^-$ macrophage subset were associated with impaired muscle regeneration. Because these events occurred with early DT ablation, it is not fully evident which cellular event, surge of monocytes at days 4 and 5 or depletion of macrophages and altered subtype distribution on recovery, was the predominant cause of the impair muscle regeneration phenotype. However, we have explored monocyte/macrophage recruitment-deficient models of impaired skeletal muscle regeneration such as the *Ccr2*$^{-/-}$ mice.[22] The impaired regeneration phenotype was very similar to the early DT-ablated CD11b-DTR mouse; however, the monocyte surge did not occur, suggesting the essential cellular event was macrophage ablation, an attribute shared by both models.

Further support for the beneficial role of Ly6C$^-$ monocytes/macrophages and the importance of the orderly macrophage subtype transition in muscle regeneration has been described in several publications. Thrombospondin-1 (*Tsp1*) regulates the release of proinflammatory and anti-inflammatory cytokines,[74] and was highly expressed during various models of tissue injury.[75,76] In a hindlimb ischemia model, *Tsp1*$^{-/-}$ mice recruited similar numbers of total macrophages, but had an increased ratio of Ly6C$^-$ to Ly6C$^+$ macrophages, resulting in decreased necrosis with increased angiogenesis and muscle regeneration compared to controls.[55] Mitogen-activated protein kinase phosphatase-1 (MKP-1), a negative regulator of MAPKs (p38 and JNK),[77] plays a role in muscle regeneration[78] and innate immunity.[79] Loss of MKP-1 deregulated the timely transition of macrophage from a proinflammatory Ly6C$^+$ to anti-inflammatory Ly6C$^-$ state, resulting in impaired muscle regeneration, suggesting that orchestrated macrophage-phenotype transition controlled by MKP-1 is critical to muscle regeneration.[72] Other compelling evidence for the essential role of anti-inflammatory macrophages has been provided by a mouse model with deletion of two cAMP response element-binding (CREB)-binding sites from the CCAAT/enhancer-binding protein beta (Cebpb) promoter. Although the macrophage recruitment and proinflammatory macrophage gene phenotype were normal, anti-inflammatory macrophage polarization was defective, evidenced by a failure of induction of the M2-specific gene *Arg1*. Mice with the mutated Cebpb promoter removed necrotic muscle but had severe defects in muscle fiber regeneration.[12] Lu et al[23] reported diminished Ly6C$^+$ and Ly6C$^-$ populations in injured skeletal muscle of *Ccl2*$^{-/-}$ mice and that muscle macrophages exhibited diminished IGF-1 expression at day 3 following injury in *Ccl2*$^{-/-}$ compared to wild-type mice. Supplementation of IGF-1 *in vivo* at day 3 recovered skeletal muscle regeneration in *Ccl2*$^{-/-}$ mice. It is possible that IGF-1 deficiency, potentially due to the decrease in Ly6C$^-$CD301$^-$ cells in ablated mice, was one of the factors in the impaired muscle regeneration present in our model. These results support the essential role of the anti-inflammatory Ly6C$^-$ macrophages in skeletal muscle regeneration.

Although CD301 and CD206 are widely used as M2 surface markers in other tissue,[80,81] minimal expression of CD301 and CD206 was present on the CD11b$^+$F4/80$^+$ macrophages as well as other noninflammatory cells in muscle, as previously reported.[82] Surface markers for macrophage subsets can vary with the injury model and tissue being studied. Approximately 10% to 15% of the cells isolated from muscle were CD301$^+$ and CD206$^+$, with many of these cells (60% to 97%, depending on time point) being negative for CD11b (data not shown). The antibodies for CD206 and CD301 exhibited high expression in *in vitro*–polarized BM-derived macrophages exposed to IL-4 (data not shown), thus it is unlikely that the antibodies did not recognize the antigens in injured skeletal muscle. In addition, CD206 can be regulated by tissue microenvironment[83] and hormones.[84] For example, dermal mononuclear cells exhibited an increased surface expression of CD206 on migration to lymph nodes or cultured with conditioned medium from skin-explant culture.[83] Li et al[84] demonstrated that female mice exhibited enhanced surface expression of CD301 in Coxsackievirus B3–induced myocarditis, whereas male mice showed minimal surface expression, which may account for the minimal surface expression of these two markers in the male CD11b-DTR mice used in this study. Lin et al[3] demonstrated that although Ly6C^{hi} and Ly6C^{lo} flow-sorted kidney macrophages exhibited equivalent surface expression of CD206, the Ly6C^{hi} population expressed high levels of the M1-associated cytokine mRNAs *Mip-2* and *Il-1β*, and the Ly6C^{lo} population expressed M2-associated mRNAs *Igf-1*, *Ccl17*, *Ccl22*, and *Pdgf-β*. In contrast to the relative paucity of CD301 in our system, the Ly6C$^-$CD301$^-$ population exhibited arginase activity consistent with M2 macrophages *in vitro*. Recent *in vitro* studies suggest that arginase as a marker of M2 macrophages is context-dependent and that other pathways independent of the M2-related STAT6 activation can also promote the expression of arginase.[85–89] However, in the context of regenerating skeletal muscle, the utility of arginase in characterizing M2-like macrophages has been established. A recent study by Mounier et al[90] showed that loss of function of *Ampkα1* in skeletal muscle resulted in a defect of acquiring a M2 phenotype, and the *Ampkα1*$^{-/-}$ mice exhibited a decreased number of M2 marker arginase-positive cells; the number of other M2 marker (TGFβ, CD206, CD163) positive cells were increased in *Ampkα1*$^{-/-}$ mice. Additional evidence emanates from *Cebpβ* promoter mutated mice that had impaired skeletal muscle regeneration. Macrophages *in vitro* from these mice exhibited a defect in M2 macrophage-specific gene expression (*Msr1*, *Il10*, *Il13ra*, and *Arg1*), but in the animal during skeletal muscle regeneration, the evidence of a defect in M2 polarization was evident by a diminished *Arg1* expression only.[12] We characterized the Ly6C$^+$CD301$^-$ population as proinflammatory

based on the cytokine and chemokines production anticipated from M1 macrophages such as IL-1α,[46,47] MCP-1,[48–51] MCP-3,[50,51] MIP-2,[3] OSM,[52] TNFα,[7,47,49,53] and VEGF.[5,54] The additional cytokines that were significantly elevated in the Ly6C$^+$CD301$^-$ (FGF9, lymphotactin, and SCF) are not commonly associated with M1 macrophages. However, we confirmed that these three cytokines were expressed at higher levels in the cell culture supernatants of IFNγ + lipopolysaccharide–stimulated BM-derived macrophages relative to control, IL-4–stimulated, and IL-10–stimulated BM-derived macrophages (unpublished data). These findings are consistent with previous work that defined Ly6C$^+$ macrophages as proinflammatory and Ly6C$^-$ macrophages as anti-inflammatory based on cytokine production and arginase activity.[3,5,8,10]

IL-4 and IL-10 are important cytokines that are associated with M2 macrophages. For example, eosinophil-derived IL-4 in adipose tissue can sustain M2 macrophages to maintain glucose homeostasis.[91] In skeletal muscle, IL-4 secreted by eosinophils stimulated FAPs instead of macrophages to promote skeletal muscle regeneration.[92] IL-4 was not detected in our sorted macrophage populations, which may be explained by eosinophils providing the main source of IL-4. In addition, IL-10, a context-dependent cytokine,[88,93] exhibited comparable expression in both Ly6C$^+$ and Ly6C$^-$ macrophages, which is consistent with the studies performed in liver and kidney injury models.[3,6] All these findings suggest that translation of the markers of macrophage heterogeneity identified from *in vitro* to *in vivo* studies is challenging.

In conclusion, the present study defined time points when ablating monocytes/macrophages resulted in an impaired muscle regeneration phenotype. Early ablation (days 0 to 2) resulted in the most severe impairments, whereas late ablation (day 4) had minimal effects. Arnold et al[7] established the patterns of Ly6C$^+$/CX3CR1^{hi} and Ly6C$^-$/CX3CR1^{lo} monocyte/macrophage subset dynamics during skeletal muscle regeneration; however, the effects that early ablation has on the distribution of these monocyte/macrophage subsets has not been explored. Comprehensive profiling of monocyte/macrophage recruitment with early ablation suggested that monocytes recruited to injured muscle contained both Ly6C$^+$ and Ly6C$^-$ populations. We explored the dynamics of monocytes both in number and in distribution of Ly6C populations in the BM, spleen, and blood during skeletal muscle regeneration. Our studies sought to extend the definition of macrophage subsets by investigating M2 macrophage markers (CD301 and CD206) and their relation to the Ly6C populations but discovered in our model of skeletal muscle regeneration that few macrophages were positive for CD301 or CD206. Macrophages were sequentially expressed as Ly6C$^+$CD301$^-$ or double-negative cells. Ablation resulted in exaggerated monocyte recruitment and reduction in double-negative macrophages that did not attain the peak levels present in DTm control mice. To confirm that the double-negative macrophages represented an anti-inflammatory subtype, cytokine production and arginase activity were determined and provided evidence of a M2-like phenotype. The switch of macrophage subsets appears to be critical to skeletal muscle regeneration. Additional studies are required to define the precise mechanisms that control the switch of macrophage subsets, which may be used as potential therapeutic approach to promote skeletal muscle regeneration.

Acknowledgments

We acknowledge the expert assistance of Dr. Joel Michalek and Ken Ouyang in performing statistical analyses for these studies.

Supplemental Data

Supplemental material for this article can be found at *http://dx.doi.org/10.1016/j.ajpath.2013.12.020*.

References

1. Summan M, Warren GL, Mercer RR, Chapman R, Hulderman T, Van Rooijen N, Simeonova PP: Macrophages and skeletal muscle regeneration: a clodronate-containing liposome depletion study. Am J Physiol Regul Integr Comp Physiol 2006, 290:R1488–R1495
2. Tidball JG, Villalta SA: Regulatory interactions between muscle and the immune system during muscle regeneration. Am J Physiol Regul Integr Comp Physiol 2010, 298:R1173–R1187
3. Lin SL, Castano AP, Nowlin BT, Lupher ML Jr, Duffield JS: Bone marrow Ly6C^{high} monocytes are selectively recruited to injured kidney and differentiate into functionally distinct populations. J Immunol 2009, 183:6733–6743
4. Geissmann F, Jung S, Littman D: Blood monocytes consist of two principal subsets with distinct migratory properties. Immunity 2003, 19:71–82
5. Swirski F, Nahrendorf M, Etzrodt M, Wildgruber M, Cortez-Retamozo V, Panizzi P, Figueiredo JL, Kohler R, Chudnovskiy A, Waterman P, Aikawa E, Mempel T, Libby P, Weissleder R, Pittet M: Identification of splenic reservoir monocytes and their deployment to inflammatory sites. Science 2009, 325:612–616
6. Ramachandran P, Pellicoro A, Vernon MA, Boulter L, Aucott RL, Ali A, Hartland SN, Snowdon VK, Cappon A, Gordon-Walker TT, Williams MJ, Dunbar DR, Manning JR, van Rooijen N, Fallowfield JA, Forbes SJ, Iredale JP: Differential Ly-6C expression identifies the recruited macrophage phenotype, which orchestrates the regression of murine liver fibrosis. Proc Natl Acad Sci U S A 2012, 109:E3186–E3195
7. Arnold L, Henry A, Poron F, Baba-Amer Y, van Rooijen N, Plonquet A, Gherardi RK, Chazaud B: Inflammatory monocytes recruited after skeletal muscle injury switch into antiinflammatory macrophages to support myogenesis. J Exp Med 2007, 204:1057–1069
8. Nahrendorf M, Swirski FK, Aikawa E, Stangenberg L, Wurdinger T, Figueiredo JL, Libby P, Weissleder R, Pittet MJ: The healing myocardium sequentially mobilizes two monocyte subsets with divergent and complementary functions. J Exp Med 2007, 204:3037–3047
9. Leimgruber A, Berger C, Cortez-Retamozo V, Etzrodt M, Newton A, Waterman P, Figueiredo JL, Kohler R, Elpek N, Mempel T, Swirski F, Nahrendorf M, Weissleder R, Pittet M: Behavior of endogenous tumor-associated macrophages assessed in vivo using a functionalized nanoparticle. Neoplasia 2009, 11:459–468

10. Dunay IR, Damatta RA, Fux B, Presti R, Greco S, Colonna M, Sibley LD: Gr1(+) inflammatory monocytes are required for mucosal resistance to the pathogen Toxoplasma gondii. Immunity 2008, 29: 306–317
11. Serbina N, Hohl T, Cherny M, Pamer E: Selective expansion of the monocytic lineage directed by bacterial infection. J Immunol 2009, 183:1900–1910
12. Ruffell D, Mourkioti F, Gambardella A, Kirstetter P, Lopez R, Rosenthal N, Nerlov C: A CREB-C/EBPbeta cascade induces M2 macrophage-specific gene expression and promotes muscle injury repair. Proc Natl Acad Sci U S A 2009, 106:17475–17480
13. Carlin LM, Stamatiades EG, Auffray C, Hanna RN, Glover L, Vizcay-Barrena G, Hedrick CC, Cook HT, Diebold S, Geissmann F: Nr4a1-Dependent Ly6C(low) Monocytes Monitor Endothelial Cells and Orchestrate Their Disposal. Cell 2013, 153:362–375
14. Brigitte M, Schilte C, Plonquet A, Baba-Amer Y, Henri A, Charlier C, Tajbakhsh S, Albert M, Gherardi R, Chrétien F: Muscle resident macrophages control the immune cell reaction in a mouse model of notexin-induced myoinjury. Arthritis Rheum 2010, 62: 268–279
15. Cailhier JF, Partolina M, Vuthoori S, Wu S, Ko K, Watson S, Savill J, Hughes J, Lang RA: Conditional macrophage ablation demonstrates that resident macrophages initiate acute peritoneal inflammation. J Immunol 2005, 174:2336–2342
16. Tidball JG, Wehling-Henricks M: Macrophages promote muscle membrane repair and muscle fibre growth and regeneration during modified muscle loading in mice in vivo. J Physiol 2007, 578: 327–336
17. Brickson S, Ji LL, Schell K, Olabisi R, St Pierre Schneider B, Best TM: M1/70 attenuates blood-borne neutrophil oxidants, activation, and myofiber damage following stretch injury. J Appl Physiol 2003, 95:969–976
18. Zerria K, Jerbi E, Hammami S, Maaroufi A, Boubaker S, Xiong JP, Arnaout MA, Fathallah DM: Recombinant integrin CD11b A-domain blocks polymorphonuclear cells recruitment and protects against skeletal muscle inflammatory injury in the rat. Immunology 2006, 119:431–440
19. Segawa M, Fukada S, Yamamoto Y, Yahagi H, Kanematsu M, Sato M, Ito T, Uezumi A, Hayashi S, Miyagoe-Suzuki Y, Takeda S, Tsujikawa K, Yamamoto H: Suppression of macrophage functions impairs skeletal muscle regeneration with severe fibrosis. Exp Cell Res 2008, 314:3232–3244
20. Ochoa O, Sun D, Reyes-Reyna SM, Waite LL, Michalek JE, McManus LM, Shireman PK: Delayed angiogenesis and VEGF production in CCR2-/- mice during impaired skeletal muscle regeneration. Am J Physiol Regul Integr Comp Physiol 2007, 293:R651–R661
21. Shireman PK, Contreras-Shannon V, Ochoa O, Karia BP, Michalek JE, McManus LM: MCP-1 deficiency causes altered inflammation with impaired skeletal muscle regeneration. J Leukoc Biol 2007, 81:775–785
22. Martinez CO, McHale MJ, Wells JT, Ochoa O, Michalek JE, McManus LM, Shireman PK: Regulation of skeletal muscle regeneration by CCR2-activating chemokines is directly related to macrophage recruitment. Am J Physiol Regul Integr Comp Physiol 2010, 299:R832–R842
23. Lu H, Huang D, Ransohoff RM, Zhou L: Acute skeletal muscle injury: CCL2 expression by both monocytes and injured muscle is required for repair. FASEB J 2011, 25:3344–3355
24. Lu H, Huang D, Saederup N, Charo I, Ransohoff R, Zhou L: Macrophages recruited via CCR2 produce insulin-like growth factor-1 to repair acute skeletal muscle injury. FASEB J 2011, 25:358–369
25. Sun D, Martinez CO, Ochoa O, Ruiz-Willhite L, Bonilla JR, Centonze VE, Waite LL, Michalek JE, McManus LM, Shireman PK: Bone marrow-derived cell regulation of skeletal muscle regeneration. FASEB J 2009, 23:382–395
26. Martinez FO, Sica A, Mantovani A, Locati M: Macrophage activation and polarization. Front Biosci 2008, 13:453–461
27. Mosser D, Edwards J: Exploring the full spectrum of macrophage activation. Nat Rev Immunol 2008, 8:958–969
28. Hume DA: Differentiation and heterogeneity in the mononuclear phagocyte system. Mucosal Immunol 2008, 1:432–441
29. Geissmann F, Manz MG, Jung S, Sieweke MH, Merad M, Ley K: Development of monocytes, macrophages, and dendritic cells. Science 2010, 327:656–661
30. Bacci M, Capobianco A, Monno A, Cottone L, Di Puppo F, Camisa B, Mariani M, Brignole C, Ponzoni M, Ferrari S, Panina-Bordignon P, Manfredi A, Rovere-Querini P: Macrophages are alternatively activated in patients with endometriosis and required for growth and vascularization of lesions in a mouse model of disease. Am J Pathol 2009, 175:547–556
31. Prokop S, Heppner FL, Goebel HH, Stenzel W: M2 polarized macrophages and giant cells contribute to myofibrosis in neuromuscular sarcoidosis. Am J Pathol 2011, 178:1279–1286
32. Chazaud B, Brigitte M, Yacoub-Youssef H, Arnold L, Gherardi R, Sonnet C, Lafuste P, Chretien F: Dual and beneficial roles of macrophages during skeletal muscle regeneration. Exerc Sport Sci Rev 2009, 37:18–22
33. McLennan IS: Degenerating and regenerating skeletal muscles contain several subpopulations of macrophages with distinct spatial and temporal distributions. J Anat 1996, 188(Pt 1):17–28
34. St Pierre BA, Tidball JG: Differential response of macrophage subpopulations to soleus muscle reloading after rat hindlimb suspension. J Appl Physiol 1994, 77:290–297
35. Duffield JS, Forbes SJ, Constandinou CM, Clay S, Partolina M, Vuthoori S, Wu S, Lang R, Iredale JP: Selective depletion of macrophages reveals distinct, opposing roles during liver injury and repair. J Clin Invest 2005, 115:56–65
36. Mirza R, DiPietro LA, Koh TJ: Selective and specific macrophage ablation is detrimental to wound healing in mice. Am J Pathol 2009, 175:2454–2462
37. Naglich JG, Rolf JM, Eidels L: Expression of functional diphtheria toxin receptors on highly toxin-sensitive mouse cells that specifically bind radioiodinated toxin. Proc Natl Acad Sci U S A 1992, 89: 2170–2174
38. Pappenheimer AM Jr, Harper AA, Moynihan M, Brockes JP: Diphtheria toxin and related proteins: effect of route of injection on toxicity and the determination of cytotoxicity for various cultured cells. J Infect Dis 1982, 145:94–102
39. Jung S, Unutmaz D, Wong P, Sano G, De los Santos K, Sparwasser T, Wu S, Vuthoori S, Ko K, Zavala F, Pamer EG, Littman DR, Lang RA: In vivo depletion of CD11c+ dendritic cells abrogates priming of CD8+ T cells by exogenous cell-associated antigens. Immunity 2002, 17:211–220
40. Clarke MC, Figg N, Maguire JJ, Davenport AP, Goddard M, Littlewood TD, Bennett MR: Apoptosis of vascular smooth muscle cells induces features of plaque vulnerability in atherosclerosis. Nat Med 2006, 12:1075–1080
41. Cailhier JF, Sawatzky DA, Kipari T, Houlberg K, Walbaum D, Watson S, Lang RA, Clay S, Kluth D, Savill J, Hughes J: Resident pleural macrophages are key orchestrators of neutrophil recruitment in pleural inflammation. Am J Respir Crit Care Med 2006, 173: 540–547
42. Fletcher JE, Hubert M, Wieland SJ, Gong QH, Jiang MS: Similarities and differences in mechanisms of cardiotoxins, melittin and other myotoxins. Toxicon 1996, 34:1301–1311
43. Roederer M: Spectral compensation for flow cytometry: visualization artifacts, limitations, and caveats. Cytometry 2001, 45:194–205
44. Shireman PK, Contreras-Shannon V, Reyes-Reyna SM, Robinson SC, McManus LM: MCP-1 parallels inflammatory and regenerative responses in ischemic muscle. J Surg Res 2006, 134:145–157
45. Classen A, Lloberas J, Celada A: Macrophage activation: classical versus alternative. Methods Mol Biol 2009, 531:29–43
46. Janson RW, Hance KR, King TE Jr: Human alveolar macrophages produce predominantly the 35-kD pro-forms of interleukin-1 alpha

and interleukin-1 beta when stimulated with lipopolysaccharide. Am J Respir Crit Care Med 1995, 151:1613–1620
47. Bai T, Chen CC, Lau LF: Matricellular protein CCN1 activates a proinflammatory genetic program in murine macrophages. J Immunol 2010, 184:3223–3232
48. Vinuesa E, Hotter G, Jung M, Herrero-Fresneda I, Torras J, Sola A: Macrophage involvement in the kidney repair phase after ischaemia/reperfusion injury. J Pathol 2008, 214:104–113
49. Hui KP, Lee SM, Cheung CY, Ng IH, Poon LL, Guan Y, Ip NY, Lau AS, Peiris JS: Induction of proinflammatory cytokines in primary human macrophages by influenza A virus (H5N1) is selectively regulated by IFN regulatory factor 3 and p38 MAPK. J Immunol 2009, 182:1088–1098
50. Domachowske JB, Bonville CA, Easton AJ, Rosenberg HF: Differential expression of proinflammatory cytokine genes in vivo in response to pathogenic and nonpathogenic pneumovirus infections. J Infect Dis 2002, 186:8–14
51. Aung HT, Schroder K, Himes SR, Brion K, van Zuylen W, Trieu A, Suzuki H, Hayashizaki Y, Hume DA, Sweet MJ, Ravasi T: LPS regulates proinflammatory gene expression in macrophages by altering histone deacetylase expression. FASEB J 2006, 20:1315–1327
52. Guihard P, Danger Y, Brounais B, David E, Brion R, Delecrin J, Richards CD, Chevalier S, Redini F, Heymann D, Gascan H, Blanchard F: Induction of osteogenesis in mesenchymal stem cells by activated monocytes/macrophages depends on oncostatin M signaling. Stem Cells 2012, 30:762–772
53. Mantovani A, Sica A, Sozzani S, Allavena P, Vecchi A, Locati M: The chemokine system in diverse forms of macrophage activation and polarization. Trends Immunol 2004, 25:677–686
54. Willenborg S, Lucas T, van Loo G, Knipper JA, Krieg T, Haase I, Brachvogel B, Hammerschmidt M, Nagy A, Ferrara N, Pasparakis M, Eming SA: CCR2 recruits an inflammatory macrophage subpopulation critical for angiogenesis in tissue repair. Blood 2012, 120:613–625
55. Brechot N, Gomez E, Bignon M, Khallou-Laschet J, Dussiot M, Cazes A, Alanio-Brechot C, Durand M, Philippe J, Silvestre JS, Van Rooijen N, Corvol P, Nicoletti A, Chazaud B, Germain S: Modulation of macrophage activation state protects tissue from necrosis during critical limb ischemia in thrombospondin-1-deficient mice. PLoS One 2008, 3:e3950
56. Contreras-Shannon V, Ochoa O, Reyes-Reyna SM, Sun D, Michalek JE, Kuziel WA, McManus LM, Shireman PK: Fat accumulation with altered inflammation and regeneration in skeletal muscle of CCR2-/- mice following ischemic injury. Am J Physiol Cell Physiol 2007, 292:953–967
57. Ahn GO, Brown JM: Matrix metalloproteinase-9 is required for tumor vasculogenesis but not for angiogenesis: role of bone marrow-derived myelomonocytic cells. Cancer Cell 2008, 13:193–205
58. Menke J, Iwata Y, Rabacal W, Basu R, Yeung Y, Humphreys B, Wada T, Schwarting A, Stanley R, Kelley V: CSF-1 signals directly to renal tubular epithelial cells to mediate repair in mice. J Clin Invest 2009, 119:2330–2342
59. Perides G, Weiss E, Michael E, Laukkarinen J, Duffield J, Steer M: TNF-α dependent regulation of acute pancreatitis severity by LY-6Chi monocytes in mice. J Biol Chem 2011, 286:13327–13335
60. Warren GL, Hulderman T, Mishra D, Gao X, Millecchia L, O'Farrell L, Kuziel WA, Simeonova PP: Chemokine receptor CCR2 involvement in skeletal muscle regeneration. FASEB J 2005, 19:413–415
61. Uezumi A, Fukada S, Yamamoto N, Takeda S, Tsuchida K: Mesenchymal progenitors distinct from satellite cells contribute to ectopic fat cell formation in skeletal muscle. Nat Cell Biol 2010, 12:143–152
62. Joe AW, Yi L, Natarajan A, Le Grand F, So L, Wang J, Rudnicki MA, Rossi FM: Muscle injury activates resident fibro/adipogenic progenitors that facilitate myogenesis. Nat Cell Biol 2010, 12:153–163
63. David Dong ZM, Aplin AC, Nicosia RF: Regulation of angiogenesis by macrophages, dendritic cells, and circulating myelomonocytic cells. Curr Pharm Des 2009, 15:365–379
64. Moldovan L, Moldovan NI: Role of monocytes and macrophages in angiogenesis. EXS 2005, (24):127–146
65. Tidball JG: Inflammatory processes in muscle injury and repair. Am J Physiol Regul Integr Comp Physiol 2005, 288:R345–R353
66. Toumi H, Best TM: The inflammatory response: friend or enemy for muscle injury? Br J Sports Med 2003, 37:284–286
67. Nguyen HX, Lusis AJ, Tidball JG: Null mutation of myeloperoxidase in mice prevents mechanical activation of neutrophil lysis of muscle cell membranes in vitro and in vivo. J Physiol 2005, 565: 403–413
68. Amano H, Morimoto K, Senba M, Wang H, Ishida Y, Kumatori A, Yoshimine H, Oishi K, Mukaida N, Nagatake T: Essential contribution of monocyte chemoattractant protein-1/C-C chemokine ligand-2 to resolution and repair processes in acute bacterial pneumonia. J Immunol 2004, 172:398–409
69. Li P, Garcia GE, Xia Y, Wu W, Gersch C, Park PW, Truong L, Wilson CB, Johnson R, Feng L: Blocking of monocyte chemoattractant protein-1 during tubulointerstitial nephritis resulted in delayed neutrophil clearance. Am J Pathol 2005, 167:637–649
70. van Furth R, Cohn ZA: The origin and kinetics of mononuclear phagocytes. J Exp Med 1968, 128:415–435
71. Ingersoll MA, Platt AM, Potteaux S, Randolph GJ: Monocyte trafficking in acute and chronic inflammation. Trends Immunol 2011, 32: 470–477
72. Perdiguero E, Sousa-Victor P, Ruiz-Bonilla V, Jardi M, Caelles C, Serrano AL, Munoz-Canoves P: p38/MKP-1-regulated AKT coordinates macrophage transitions and resolution of inflammation during tissue repair. J Cell Biol 2011, 195:307–322
73. Jenkins SJ, Ruckerl D, Cook PC, Jones LH, Finkelman FD, van Rooijen N, MacDonald AS, Allen JE: Local macrophage proliferation, rather than recruitment from the blood, is a signature of TH2 inflammation. Science 2011, 332:1284–1288
74. Yamauchi Y, Kuroki M, Imakiire T, Abe H, Uchida H, Beppu R, Yamashita Y, Shirakusa T: Thrombospondin-1 differentially regulates release of IL-6 and IL-10 by human monocytic cell line U937. Biochem Biophys Res Commun 2002, 290:1551–1557
75. Agah A, Kyriakides TR, Lawler J, Bornstein P: The lack of thrombospondin-1 (TSP1) dictates the course of wound healing in double-TSP1/TSP2-null mice. Am J Pathol 2002, 161:831–839
76. Lawler J: Thrombospondin-1 as an endogenous inhibitor of angiogenesis and tumor growth. J Cell Mol Med 2002, 6:1–12
77. Owens DM, Keyse SM: Differential regulation of MAP kinase signalling by dual-specificity protein phosphatases. Oncogene 2007, 26: 3203–3213
78. Shi H, Boadu E, Mercan F, Le AM, Flach RJ, Zhang L, Tyner KJ, Olwin BB, Bennett AM: MAP kinase phosphatase-1 deficiency impairs skeletal muscle regeneration and exacerbates muscular dystrophy. FASEB J 2010, 24:2985–2997
79. Chi H, Barry SP, Roth RJ, Wu JJ, Jones EA, Bennett AM, Flavell RA: Dynamic regulation of pro- and anti-inflammatory cytokines by MAPK phosphatase 1 (MKP-1) in innate immune responses. Proc Natl Acad Sci U S A 2006, 103:2274–2279
80. Fujiu K, Manabe I, Nagai R: Renal collecting duct epithelial cells regulate inflammation in tubulointerstitial damage in mice. J Clin Invest 2011, 121:3425–3441
81. Fujisaka S, Usui I, Bukhari A, Ikutani M, Oya T, Kanatani Y, Tsuneyama K, Nagai Y, Takatsu K, Urakaze M, Kobayashi M, Tobe K: Regulatory mechanisms for adipose tissue M1 and M2 macrophages in diet-induced obese mice. Diabetes 2009, 58:2574–2582
82. Jansen K, Pavlath G: Mannose receptor regulates myoblast motility and muscle growth. J Cell Biol 2006, 174:403–413
83. Dupasquier M, Stoitzner P, Wan H, Cerqueira D, van Oudenaren A, Voerman JS, Denda-Nagai K, Irimura T, Raes G, Romani N, Leenen PJ: The dermal microenvironment induces the expression of the alternative activation marker CD301/mMGL in mononuclear phagocytes, independent of IL-4/IL-13 signaling. J Leukoc Biol 2006, 80:838–849

84. Li K, Xu W, Guo Q, Jiang Z, Wang P, Yue Y, Xiong S: Differential macrophage polarization in male and female BALB/c mice infected with coxsackievirus B3 defines susceptibility to viral myocarditis. Circ Res 2009, 105:353−364
85. Qualls JE, Neale G, Smith AM, Koo MS, DeFreitas AA, Zhang H, Kaplan G, Watowich SS, Murray PJ: Arginine usage in mycobacteria-infected macrophages depends on autocrine-paracrine cytokine signaling. Sci Signal 2010, 3:ra62
86. Ben Addi A, Lefort A, Hua X, Libert F, Communi D, Ledent C, Macours P, Tilley SL, Boeynaems JM, Robaye B: Modulation of murine dendritic cell function by adenine nucleotides and adenosine: involvement of the A(2B) receptor. Eur J Immunol 2008, 38:1610−1620
87. Murray PJ, Wynn TA: Obstacles and opportunities for understanding macrophage polarization. J Leukoc Biol 2011, 89:557−563
88. Murray PJ, Wynn TA: Protective and pathogenic functions of macrophage subsets. Nat Rev Immunol 2011, 11:723−737
89. Chang CI, Zoghi B, Liao JC, Kuo L: The involvement of tyrosine kinases, cyclic AMP/protein kinase A, and p38 mitogen-activated protein kinase in IL-13-mediated arginase I induction in macrophages: its implications in IL-13-inhibited nitric oxide production. J Immunol 2000, 165:2134−2141
90. Mounier R, Theret M, Arnold L, Cuvellier S, Bultot L, Goransson O, Sanz N, Ferry A, Sakamoto K, Foretz M, Viollet B, Chazaud B: AMPKalpha1 regulates macrophage skewing at the time of resolution of inflammation during skeletal muscle regeneration. Cell Metab 2013, 18:251−264
91. Wu D, Molofsky A, Liang H-E, Ricardo-Gonzalez R, Jouihan H, Bando J, Chawla A, Locksley R: Eosinophils sustain adipose alternatively activated macrophages associated with glucose homeostasis. Science 2011, 332:243−247
92. Heredia JE, Mukundan L, Chen FM, Mueller AA, Deo RC, Locksley RM, Rando TA, Chawla A: Type 2 innate signals stimulate fibro/adipogenic progenitors to facilitate muscle regeneration. Cell 2013, 153:376−388
93. Saraiva M, O'Garra A: The regulation of IL-10 production by immune cells. Nat Rev Immunol 2010, 10:170−181